อนุภาคพอลิฟีนอลจากใบชาที่มีเฟอร์โรซีนเป็นตัวพายาต้านมะเร็ง

นายปัณณวิชญ์ ไพยริน

วิทยานิพนธ์นี้เป็นส่วนหนึ่งของการศึกษาตามหลักสูตรปริญญาวิทยาศาสตรมหาบัณฑิต
สาขาวิชาเคมี ภาควิชาเคมี
คณะวิทยาศาสตร์ จุฬาลงกรณ์มหาวิทยาลัย
ปีการศึกษา 2560

FERROCENE-BEARING TEA POLYPHENOL PARTICLES AS ANTICANCER DRUG CARRIERS

Mr. Punnawich Phaiyarin

A Thesis Submitted in Partial Fulfillment of the Requirements

for the Degree of Master of Science Program in Chemistry

Department of Chemistry

Faculty of Science

Chulalongkorn University

Academic Year 2017

Thesis Title	FERROCENE-BEARING TEA POLYPHENOL PARTICLES AS ANTICANCER DRUG CARRIERS
By	Mr. Punnawich Phaiyarin
Field of Study	Chemistry
Thesis Advisor	Professor Supason Wanichwecharungruang, Ph.D.

Accepted by the Faculty of Science, Chulalongkorn University in Partial Fulfillment of the Requirements for the Master's Degree

.....Dean of the Faculty of Science

(Associate Professor Polkit Sangvanich, Ph.D.)

THESIS COMMITTEE

.....Chairman

(Associate Professor Vudhichai Parasuk, Ph.D.)

.....Thesis Advisor

(Professor Supason Wanichwecharungruang, Ph.D.)

.....Examiner

(Associate Professor Voravee Hoven, Ph.D.)

.....External Examiner

(Kriengsak Lirdprapamongkol, Ph.D.)

ปัณณวิชญ์ ไพยริน : อนุภาคพอลิฟีนอลจากใบชาที่มีเฟอร์โรซีนเป็นตัวพายาต้านมะเร็ง (FERROCENE-BEARING TEA POLYPHENOL PARTICLES AS ANTICANCER DRUG CARRIERS) อ.ที่ปรึกษาวิทยานิพนธ์หลัก: ศ. ดร.ศุภศร วนิชเวชารุ่งเรือง, 58 หน้า.

เฟอร์โรซีนเป็นสารประกอบที่สามารถเกิดประจุบวกเมื่อถูกออกซิไดส์ การใช้เฟอร์โรซีนเป็นหมู่ติดในพอลิเมอร์อาจมีส่วนช่วยในการเพิ่มสมบัติการละลายน้ำของพอลิเมอร์ได้ ในงานวิจัยนี้ ได้เตรียมอนุภาคและพอลิเมอร์จากพอลิฟีนอลจากชา (pEGCG และ pEGCG-gum) จากพอลิฟีนอลจากชา (EGCG) จากนั้นทำการติดเฟอร์โรซีนลงบนอนุภาคและพอลิเมอร์ดังกล่าว ส่งผลให้เกิดการจัดเรียงตัวใหม่เป็นอนุภาคขนาดกึ่งไมครอน ซึ่งไม่ละลายและไม่กระจายตัวในน้ำ อนุภาคที่ติดเฟอร์โรซีน เมื่อทำปฏิกิริยากับไฮโดรเจนเปอร์ออกไซด์ เกิดเป็นอนุภาคที่กระจายตัวได้ดีในน้ำ ที่มีขนาดระดับนาโนเมตร นอกจากนี้อนุภาคออกซิไดส์พอลิฟีนอลจากชาที่ติดเฟอร์โรซีน Fc-pEG-gum สามารถยับยั้งการเจริญเติบโตของเซลล์มะเร็งตับ (HepG2 เซลล์ไลน์) ประมาณ 30 เปอร์เซนต์ที่ความเข้มข้น 100 ไมโครกรัมต่อมิลลิลิตร

ภาควิชา เคมี ลายมือชื่อนิสิต .....

สาขาวิชา เคมี ลายมือชื่อ อ.ที่ปรึกษาหลัก .....

ปีการศึกษา 2560

5871919623 : MAJOR CHEMISTRY

KEYWORDS: POLYMERIZED TEA POLYPHENOL / FERROCENE-BEARING PARTICLES / OXIDATION-RESPONSIVENESS

PUNNAWICH PHAIYARIN: FERROCENE-BEARING TEA POLYPHENOL PARTICLES AS ANTICANCER DRUG CARRIERS. ADVISOR: PROF. SUPASON WANICHWECHARUNGRUANG, Ph.D., 58 pp.

Ferrocene is a redox moiety that can be positively charged upon being oxidized. Thus, it is possible to use this moiety to make a polymer platform that is redox responsive regarding their water solubility. Here we prepared polymerized EGCG nanoparticles (pEGCG) and polymerized EGCG gum (pEGCG-gum) from tea polyphenol EGCG. Ferrocene was grafted onto the polymerized tea polyphenol and the obtained polymers were allowed to self-assemble into water-insoluble and indispersible sub-micron particles. The water-insoluble ferrocene-bearing particles became water-dispersible particles with nanometer sizes upon being oxidized by hydrogen peroxide. The oxidized particles, Fc-pEG-gum can inhibit growth of HepG2 liver cancer cells about 30 percentage at 100 μg/mL.

Department: Chemistry
Field of Study: Chemistry
Academic Year: 2017

Student's Signature .....

Advisor's Signature .....

ACKNOWLEDGEMENTS

I would first like to thank my thesis advisor Prof. Dr. Supason Wanichwecharungruang of the department of Chemistry, faculty of science at Chulalongkorn university. The door to Prof. Wanichwecharungruang office was always open whenever I ran into a trouble spot or had a question about my research or writing. She consistently allowed this paper to be my own work but steered me in the right the direction whenever she thought I needed it. I also gratefully acknowledge all the committees for their comment and suggestions of my works. I would also like to thank the experts who were involved in the anti-cancer activity evaluation for this research project: Miss Thitiporn Pattarakankul, Dr. Kriengsak Lirdprapamongkol, without their passionate participation and input, the anti-cancer activity evaluation could not have been successfully conducted. I would also like to thank all of my friends and SW lab members for any helps Finally, I must express my very profound gratitude to my parents for providing me with unfailing support and continuous encouragement throughout my years of study and through the process of researching and writing this thesis. This accomplishment would not have been possible without them.

CONTENTS

Page

Page

LIST OF TABLE

Page

LIST OF FIGURE

Page

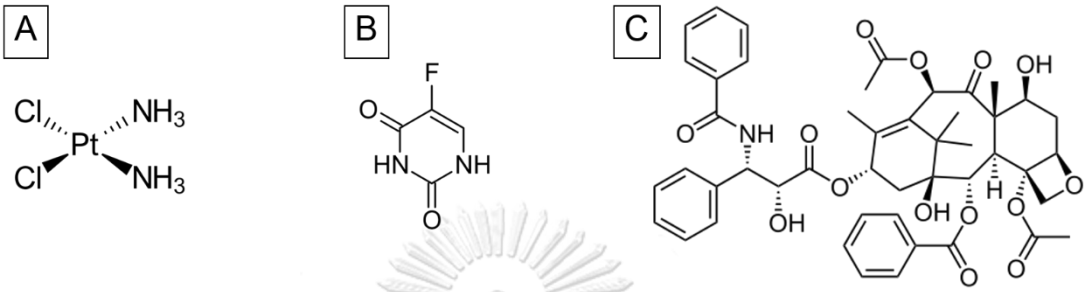

CHAPTER I

INTRODUCTION

1.1 Cancer and Treatment

Cancer is the out of control growth of abnormal cells. Cancer cells can accumulate to form a dense pack of cell called ‘tumor’. Cancer cells can spread to other parts of the body. Wilailak et al. [1] reported new 100,000 cancer patients in 2011, of which liver and breast cancers were the most found cancer types in Thailand. At present, there are 3 approaches for cancer treatment, surgery [2], radiotherapy [3], and chemotherapy [4]. In this work, we are interested in chemotherapy. There are many drugs to treat cancer through different mechanisms of action, for example, cisplatin exert its activity by blocking DNA duplication [5], 5-fluorouracil works by blocking the action of thymidylate synthase [6] and paclitaxel acts by interfering with the normal function of microtubules during cell division [7]. Nevertheless, these drugs act in both normal and cancer cells, thus causing various toxic side-effects, such as nausea, vomiting, and fatigue [8, 9].

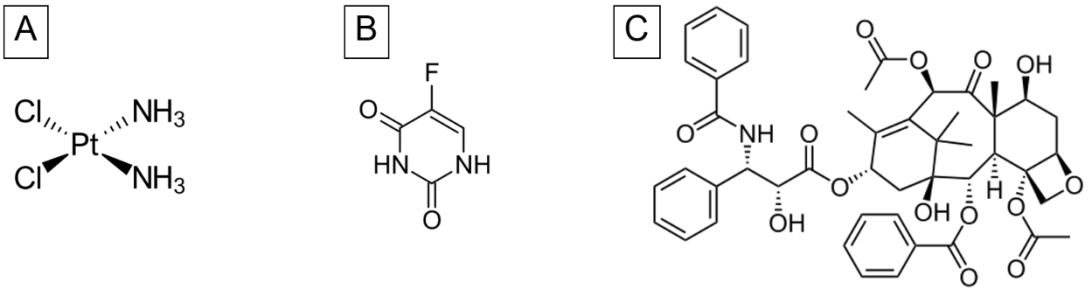

Figure 1.1 Chemical structure of anti-cancer drugs (A) Cisplatin (B) 5-Fluorouracil and (C) Paclitaxel

1.2 Nanoparticles Drug Delivery Systems for Cancer Therapies

Drug delivery system is the approaches that can increase the bioavailability of water-insoluble drugs, prolong sustainable drug release and deliver drugs to the target sites [10]. Recently anti-cancer drug delivery system has been developed by modification the carriers with moieties that were responsive to either endogenous stimuli such as, pH [11, 12] and redox gradient [13] or exogenous stimuli such as, light [14], temperature [15] and magnetic field [16]. Many in vitro studies of stimuli-responsive drug delivery system showed promising results in cancer cells few have been tested in in vivo and clinical stage. Drug carriers that have been designed to go specifically to only cancer cells although gave success in an initial treatment stage, usually showed resistant later on [17].

1.3 Natural Product

In drug discovery process, many bioactive compounds were discovered from natural sources, i.e. plants and animals. These bioactive molecules are produced via secondary metabolism [18, 19], for example, caffeine, alkaloid compound are from cocoa, coffee,

and tea [20]. Paclitaxel is an anti-cancer drug extracted from *Taxus brevifola* [21] which has been approved for medical use in human [22]. Another interesting anti-cancer compound is tea polyphenol. The major phenolic compound in tea is catechin, i.e. epicatechin (EC), epigallocatechin (EGC), epicatechin-3-gallate (ECG) and epigallocatechin-3-gallate (EGCG) [23, 24].

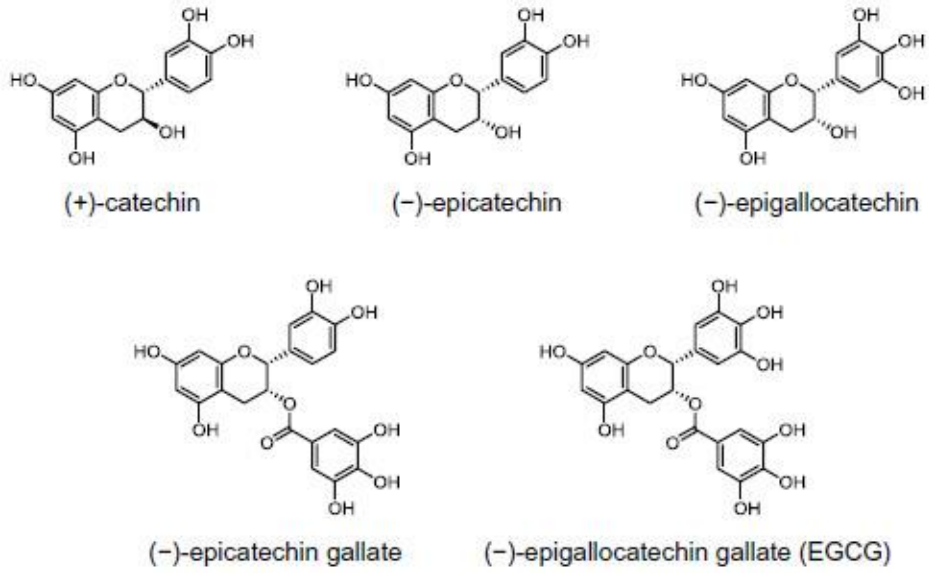

Figure 1.2 Chemical structures of tea catechins [25]

1.4 Epigallocatechin-3-gallate (EGCG)

Among tea catechins, epigallocatechin-3-gallate or EGCG is the most abundant in tea leaves [26, 27]. EGCG is a phenolic compound with flavan-3-ol core structure, it is an ester of gallic acid and epigallocatechin. EGCG contains many hydroxy groups in the structure, thus it is well soluble in water. EGCG exhibits various bioactivities including osteoporosis prevention [28], improving dental health [29], antioxidant activity, anti-inflammatory [30] and also anti-cancer activity [31-33].

1.5 Literature Review of EGCG Anti-Cancer Activity

In 2002, Wang *et al.* [34] studied the growth inhibitory effects of EGCG in transformed NIH-pATM*ras* fibroblasts by determining the level of ornithine decarboxylase (ODC, EC 4.1.1.17), which is a signal for cellular proliferation. The results showed a lower ODC level in the transformed cell than in the normal fibroblasts, indicating the strong growth inhibitory effects of EGCG in transformed fibroblasts but not in normal cells.

In 2012, Du *et al.* [35] compared cancer cell (HCT-116 and SW-480 human colorectal cancer cells) anti-proliferation activity of 10 polyphenolic compounds (caffeic acid, CA; gallic acid, GA; catechin, C; EC; gallocatechin, GC; CG; gallocatechin gallate, GCG; ECG; EGC; and EGCG) using MTS assay. The results showed that EGCG exhibited the most potent antiproliferative effect. They also showed that cell proliferation was decreased significantly for EGCG compared to EGC. Therefore, gallate ester moiety enhances the antiproliferative effect.

In 2016, Kwak *et al.* [36] studied the effect of EGCG on cell proliferation, migration and invasion using human cholangiocarcinoma cells (HuCC-T1) by western blot technique and wound healing assay. The results revealed that EGCG induced apoptosis at 5 μg/mL in HuCC-T1 but did in normal cells (Human embryonic kidney cells, HEK-293). EGCG also dose-dependently inhibited matrix metalloproteinase (MMP)-2/9 activity, which has a crucial role in cancer cells invasion and migration.

1.6 Polymerized EGCG

Fermented tea or semi-fermented tea include oolong and black tea. During fermentation, oxidation and polymerization of constituents usually take place [37]. The products from oxidation are oligomers of tea polyphenols which are found mainly in fermented tea. The example of oxidized products formed by tea fermentation is theaflavin and thearubigin which exhibit better anti-cancer activity than tea catechins such as, EGCG [38].

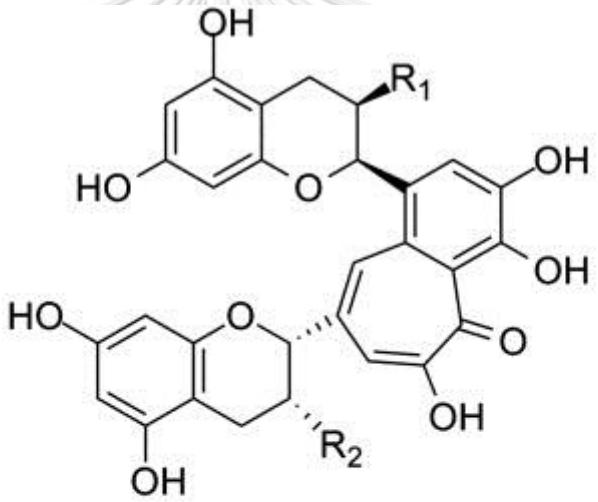

Theaflavins	R_1	R_2
Theaflavin	OH	OH
Theaflavin-3-gallate	Gallate	OH
Theaflavin-3'-gallate	OH	Gallate
Theaflavin-3,3'-digallate	Gallate	Gallate

Figure 1.3 Chemical Structures of theaflavin and its derivatives

1.7 Literature Review Anti-Cancer Activity of polymerized EGCG

In 2001, Pan *et al.* [39] studied the anti-cancer activity of theasinensin A, theaflavin (TF-1) and a mixture of theaflavin-3-gallate and theaflavin-3'-gallate (TF-2) by annexin V apoptosis assay. The results showed that theasinensin A, TF-1, and TF-2 exhibited higher apoptosis induction compared to EGCG. It can be concluded that oligomerization of tea polyphenol enhances anti-cancer activity.

In 2008, Babich *et al.* [40] studied antiproliferation of theaflavin-3-gallate (TF-2a) and theaflavin-3'-gallate (TF-2b) on human squamous carcinoma HSC-2 cells and human tongue squamous carcinoma CAL27 cells using neutral red cytotoxicity assay. The results revealed that TF-2a and TF-2b significantly inhibited cell proliferation in cancer cells. To elucidate the mechanism of action, the ferrous ion oxidation-xylenol orange (FOX) method was used to quantify peroxide generated from TF-2a and TF-2b. The results showed that hydrogen peroxide and superoxide anion were generated from TF-2a and TF-2b which indicated the toxicity of TF-2a and TF-ab occurred due to induction of oxidative stress.

1.8 Literature Review of EGCG and Polymerized Products as Drug Carrier

In 2014, Chung *et al.* [41] fabricated micellar nanocomplexes (MNCs) by complexing oligomerized EGCG with herceptin, anti-cancer protein, to form a micelle core and surrounding the core with EGCG-poly(ethylene glycol). *In vivo* study showed that the

MNCs selectively inhibited the growth of tumor and stayed in blood circulation longer than free herceptin.

In 2016, Liao *et al.* [42] prepared EGCG-nanoethosomes and studied the transdermal penetration of EGCG-nanoethosomes *in vitro*. The results showed that EGCG-nanoethosomes could penetrate through the mouse skin. To investigate the tumor growth inhibitory effect, docetaxel was loaded to EGCG-nanoethosomes (DT-EGCG-nanoethosomes) and the loaded particles were injected into mice. The results indicated that DT-EGCG-nanoethosomes could reduce the size of tumor after 14-day treatment.

In 2016, Pukfukdee *et al.* [43] fabricated polymerized EGCG nanoparticles (P-EGCG particles) as anti-cancer drug carrier via enzymatic template-controlled polymerization. Paclitaxel was loaded into OTP particles (PTX-loaded P-EGCG particles). The loaded P-EGCG particles exhibited lower IC_{50} than free paclitaxel in toxicity against A549 lung cancer cells using MTT assay. In addition, when compared to EGCG, P-EGCG possed lower IC_{50}.

1.9 Water-insoluble polymerized EGCG-gum

In the synthesis of P-EGCG by Pukfukdee [43], two different products were obtained, the water dispersible brown powder and the water-insoluble brownish sticky gum. The gum is the major product. This work, therefore, wants to modify the gum so that it is soluble in water and can be tested for its anti-cancer property.

1.10 Ferrocene

Ferrocene ($Fe(C_5H_5)_2$) is an organometallic compound which contains two cyclopentadienyl rings that embrace iron atom (also known as a sandwich structure [44, 45]. Ferrocene has low reduction potential (0.4 V versus standard hydrogen electrode [46]), making the compound easily oxidized into the positively charged ferrocenium ion [47]. Ferrocene has been used in anti-cancer drug delivery system as a redox moiety which is responsive to a high level of oxidizing agents in cancer cells [48, 49].

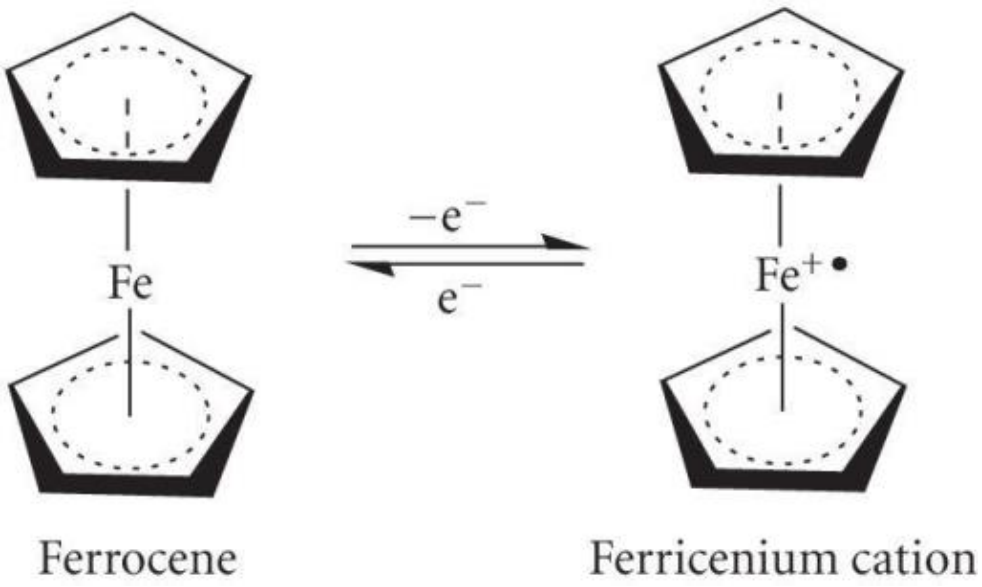

Figure 1.4 The ferrocene/ferrocenium redox couple

1.11 Literature Reviews on Oxidation-Responsiveness of Ferrocene

In 2015, Liu *et al.* [48] synthesized ferrocene-containing amphiphilic block copolymer (PEG-*b*-PMAEFc) via atom transfer radical polymerization. PEG-*b*-PMAEFc self-assembled to form polymeric micelle with rhodamine B as a drug model. Rhodamine

B released only when the material was exposed to oxidative environment. The results confirmed the oxidation-responsiveness of PEG-*b*-PMAEFc.

In 2016, Noyhouzer *et al.* [49] grafted ferrocene to phospholipid molecule to form liposome and doxorubicin was loaded as drug molecule. The results showed the selective release of doxorubicin in CCL-2 adenocarcinoma cervical cancer cells, due to the higher oxidants found in cancer cells. The drug release implied electrostatic repulsion among ferrocenium ion formed by oxidation of ferrocene moieties, thus breaking down the liposome assembly.

1.12 Objective and Scope of Work

With the above-mentioned information on the interesting anti-cancer activity of polymerized EGCG found in fermented tea and the obtained water-insoluble polymerized EGCG-gum produced by Pukfukdee [43], here we would like to introduce ferrocene moieties onto the insoluble gum structure in order to make redox-responsive polymerized EGCG. It is possible that upon oxidation, the ferrocene moieties will be ionized which could result in charged polymers that could be soluble in water.

CHAPTER II

EXPERIMENTAL

2.1 Materials and Chemicals

Epigallocatechin-3-gallate (EGCG) and horseradish peroxidase (HRP) were purchased from Chemieliva Pharmaceutical and Chemical Company (Choqqing, China). Polyethylene glycol (PEG, MW 35,000), hydrogen peroxide (H_2O_2) and iron standard solution were purchased from Merck (Darmstadt, Germany). 1-Ethyl-3-(3-dimethylaminopropyl)carbodiimide (EDCI) and *N*-hydroxysuccinimide (NHS) were purchased from Acros Organics (Geel, Belgium). Dimethylformamide (DMF) and methanol (MeOH) were purchased from RCI Labscan (Bangkok, Thailand) and ferroceneacetic acid (FAA) and paclitaxel (PTX) were purchased from TCI chemicals (Tokyo, Japan). All chemicals used were analytical grade and were used without further purification.

Freeze-drying was carried out by Freeze-dry/Shell Freeze System Model 7753501 (Labconco Corporation, Kansas, MI, USA). The infrared spectrum was obtained on germanium reflection element using a Nicolet 6700 ATR-FTIR spectrometer (Thermo Electron Corporation, Madison, WI, USA). Functional groups on the particle surface were evaluated by AXIS-ULTRA DLD XSAM800 type x-ray photoelectron spectrometer (Shimadzu/Kratos, Manchester, United Kingdom). The concentration of iron was

determined by using iCAP 7000 series Inductively coupled plasma optical emission spectrometer (Thermo Fischer Scientific, *Massachusetts, USA).* Morphology of particles was performed through JSM-7610 scanning electron microscope (JEOL, Tokyo, Japan) and transmission electron microscope coupled with energy dispersive x-ray spectrometer (JEOL, JEM-2100, Tokyo, Japan). The size distribution was obtained with Zetasizer nano series instrument (Zs, Malvern Instruments, United Kingdom). Thermal analysis of particles was required thermo gravimetric analysis (Netzsch STA 449 F1, Germany).

2.2 Synthesis of polymerized EGCG nanoparticles (pEGCG) and polymerized EGCG gum (pEGCG-gum)

pEGCG and pEGCG-gum were synthesized by Pukfukdee's protocol [43], briefly, EGCG (0.54 g), HRP (10 mg) and PEG (MW 35,000, 0.03 g) were mixed, followed by adding 3.4 mL of 8% H_2O_2, then 50% MeOH in phosphate buffer pH 7.4 was added (total volume was 18.4 mL), under vigorous stirring at room temperature for 48 h and then dialyzed against deionized water to remove leftover reagents and organic solvent, the mixture was freeze-dried to obtain brown powder pEGCG and brownish sticky pEGCG-gum respectively. %Yield of pEGCG and its gum were calculated bases on the weight of dried pEGCG or pEGCG-gum to the weight of pristine EGCG as shown in Eq. 1 below.

$$\text{Yield (\%)} = \frac{\text{weight of pEGCG (or pEGCG-gum)}}{\text{weight of EGCG}} \times 100 \qquad \text{(Eq. 1)}$$

2.3 Synthesis of ferrocene-bearing tea polyphenol particles (Fc-pEG and Fc-pEG-gum)

In this work, we used carbodiimide coupling reaction adapted from Seemork [50]. In brief, FAA (10 mg) and EDCI (38.3 mg) were dissolved in DMF and incubated at 4 °C for 30 min then NHS (23 mg) in DMF was added, followed by the addition of pEGCG (10 mg and 100 mg) and pEGCG-gum (100 mg) in DMF. The reaction was carried out overnight at room temperature, after that, the mixture was dialyzed against water to remove the leftover reagents and solvent and freeze-dried to yield black powder of ferrocene-bearing tea polyphenol particles (Fc-pEG and Fc-pEG-gum), yield percentage of products was calculated as follows: (Eq. 2, below)

$$\text{Yield (\%)} = \frac{\text{weight of Fc-pEG (or Fc-pEG-gum)}}{\text{weight of pEGCG (or pEGCG-gum)} + \text{weight of used FAA}} \times 100 \quad \text{(Eq. 2)}$$

2.4 Oxidation-responsive study of Fc-pEG and Fc-pEG-gum

To investigate the oxidation-responsive property of Fc-pEG and Fc-pEG-gum, H_2O_2 was used as an oxidizing agent, and the following method was used. The 1 M of H_2O_2 was added to Fc-pEG and Fc-pEG-gum (500 mg L^{-1}), the reaction was carried out with varied time and then dialyzed with deionized water to remove excess amount of H_2O_2, the mixture was dried by freeze-drying technique to gain yellow-green solid of oxidized Fc-pEG and Fc-pEG-gum (depicted as oxFc-pEG and oxFc-pEG-gum), and %yield was calculated as shown in Eq. 3 (below):

$$\text{Yield (\%)} = \frac{\text{weight of oxFc-pEG (or oxFc-pEG-gum)}}{\text{weight of Fc-pEG (or Fc-pEG-gum)}} \times 100 \qquad \text{(Eq. 3)}$$

2.5 Determining weight percentage of ferrocene in the particles

Percentage of ferrocene substitution degree can be calculated as follows:

$$\text{Weight percentage of ferrocene in the particles (\%)} = \frac{\text{weight of attached ferrocene}}{\text{weight of ferrocene-bearing particles}} \times 100$$

2.6 *In vitro* anti-cancer assay

In vitro anti-cancer property of products was determined [51]. oxFc-pEG, oxFc-pEG-gum, pEGCG, pEGCG-gum, EGCG and paclitaxel were tested against HepG2 liver cancer cells. MTT assay was used to evaluate the anti-cancer activity.

2.6.1 Cell line and culture conditions

The HepG2 liver cancer cells were purchased from American Type Culture Collection (ATCC, Rockville, MD, USA). The liver cancer HepG2 cells were treated in RPMI-1640 supplemented with 10% (v/v) fetal bovine serum (FBS), and 1% antibiotic (penicillin and streptomycin) in a humidified atmosphere of 5% CO_2 at 37° until confluent.

2.6.2 Determination of cell viability using MTT assay

Cell viability was calculated by the MTT (3-[4,5-methylthiazol-2-yl]-2,5-diphenyltetrazolium bromide) assay. Briefly, HepG2 cell suspensions in completed medium (5 x 10^3 cells/well) were seeded in 96-well plate containing 100 µL of culture medium and grew under humidified atmosphere for 24 h (37°, 5% CO_2) After 24 h, 100 µL of additional medium containing tested products was added to each well and cells

were allowed to grow for 72 h (37°, 5% CO_2). Then, the wells were replaced with new medium containing 0.5 mg/mL MTT and then incubated for 4 h. After that, the medium in each well was removed and 100 µL DMSO was added to dissolve the pellet (MTT metabolic product). The absorbance of the wells was measured at 550 nm (maximum absorbance of the pellet) using microplate reader and subtracted with absorbance at 650 nm which corresponded to the yellow color of initial MTT reagent. The number of viable cells can be determined as %cell viability (Eq. 4) and IC_{50} was calculated by nonlinear regression.

$$\text{Cell viability (\%)} = \frac{\text{O.D. of control-O.D. of tested product}}{\text{O.D. of control}} \times 100 \qquad \text{(Eq. 4)}$$

Where O.D. is the optical density

CHAPTER III

RESULTS AND DISCUSSION

3.1 Synthesis of pEGCG and pEGCG-gum

Starting with EGCG (Figure 3.1), using Pukfukdee protocol via the template-controlled polymerization with PEG as template and horseradish peroxidase and hydrogen peroxide as oxidizing agent, we could synthesize two polymerized EGCG materials, the water dispersible pEGCG and the water-indispersible pEGCG-gum (Figure 3.2). The yields were 4.1% and 5.7% for pEGCG and pEGCG-gum, respectively. Charaterization of pEGCG by TEM revealed the spherical-shaped particles with size around 250±20 nm (Figure 3.3). The pEGCG-gum is brownish and insoluble in hexane, dichloromethane (CH_2Cl_2), chloroform ($CHCl_3$), ethyl acetate (EtOAc), MeOH, ethanol (EtOH), acetone and deionized water (DI water) but clearly dissolved in DMF and dimethyl sulfoxide (DMSO), as shown in Figure 3.4. In this work, our aim is to introduce oxidation responsive moieties onto the two polymer chains so that they became oxidation responsive materials. We selected ferrocene as oxidation responsive moieties because the moiety will be changed upon oxidation.

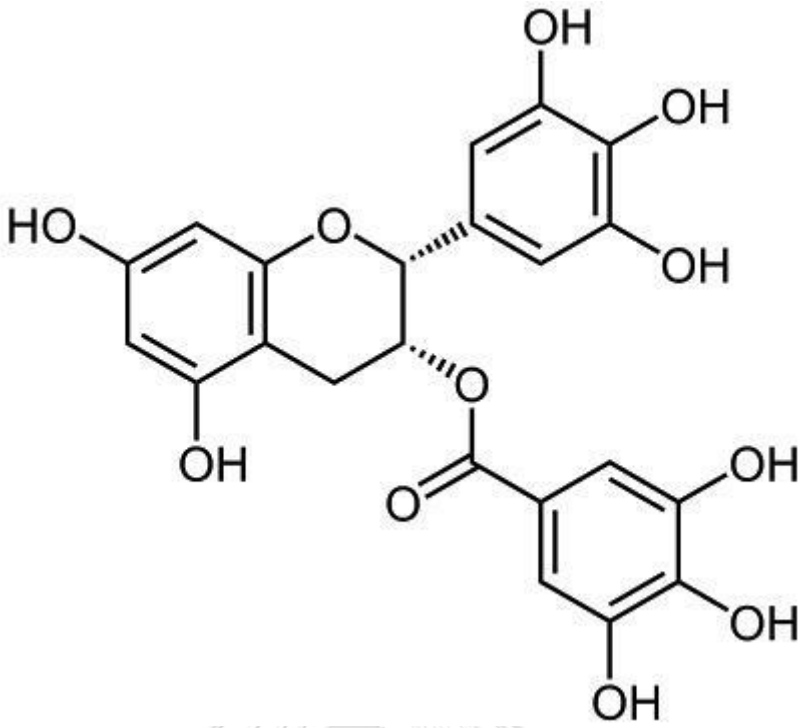

Figure 3.1 Chemical structure of EGCG

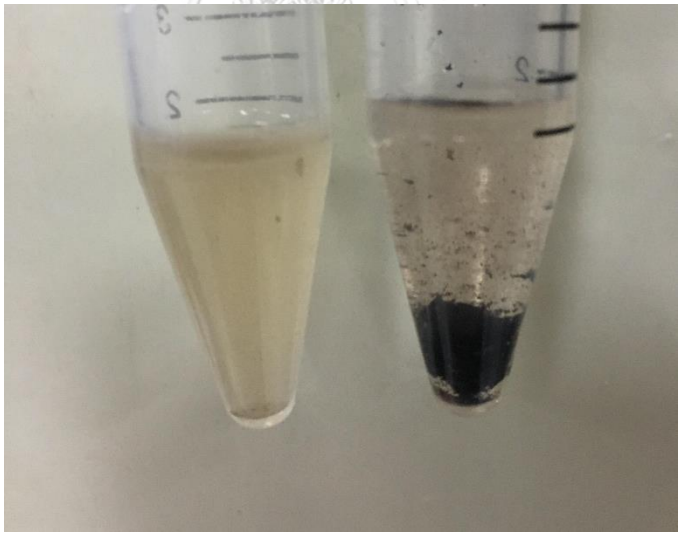

Figure 3.2 Water dispersibility of pEGCG (left) and pEGCG-gum (right)

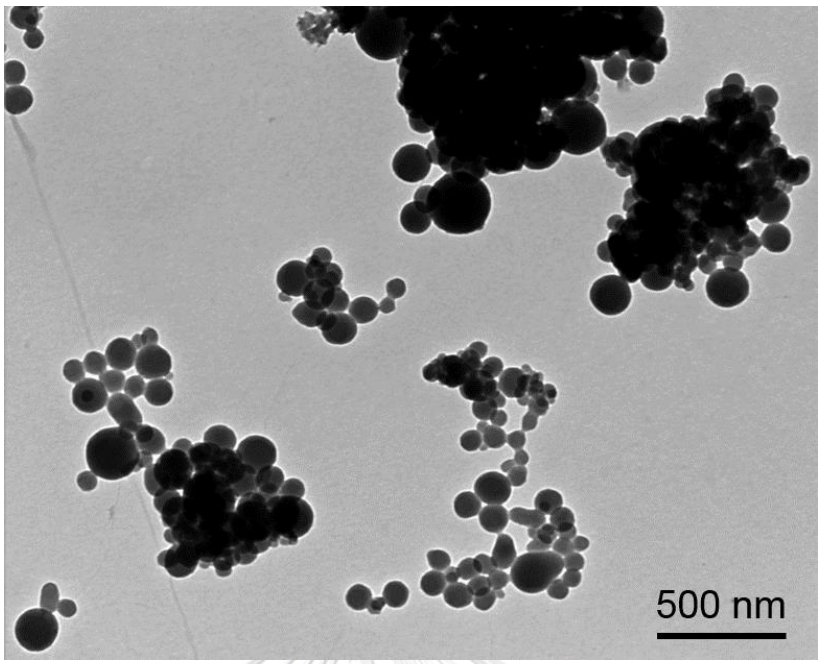

Figure 3.3 TEM image of pEGCG

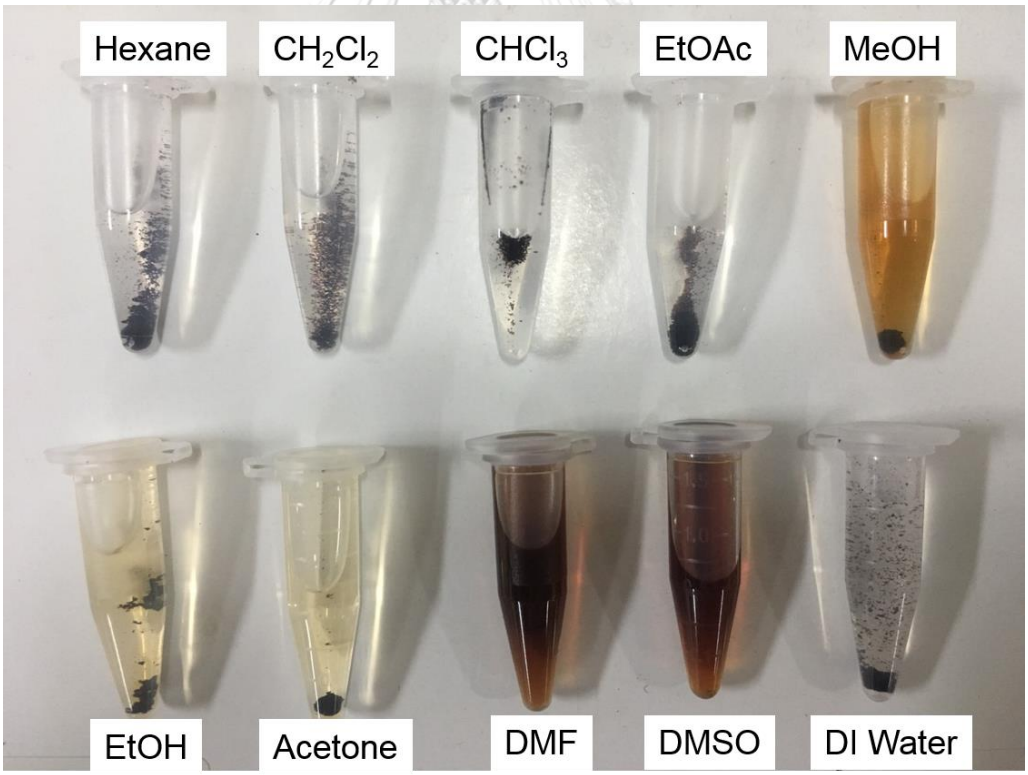

Figure 3.4 Solubility test of pEGCG-gum in various solvent

3.2 Synthesis of Fc-pEG and Fc-pEG-gum

Ferrocene moieties were grafted onto pEGCG by carbodiimide formation using EDCI and NHS as coupling agents. The reaction between ferroceneacetic acid (FAA) and pEGCG was carried out overnight. Then the mixture was dialyzed against water. In order to study the effect of amount of grafted ferrocene, we performed the synthesis under two ferrocene to pEGCG weight ratios. The product with higher weight percent of ferrocene (19.77%) was obtained from the synthesis carried out at FAA:pEGCG of 1:1 weight ratio (Table 3.1, row 1). The product with weight percent of ferrocene (4.52%) was obtained from the synthesis carried out at FAA:pEGCG of 0.1:1 weight ratio (Table 3.1, row 2). The products with higher weight percent of ferrocene in the product (Fc-pEG I) and the lower weight percent of ferrocene in the product (Fc-pEG II) were subjected to SEM and TEM analyses (Figure 3.5). The Fc-pEG I and Fc-pEG II were spherical. The size of Fc-pEG I and Fc-pEG II were around 200±20 nm and 200±50 nm, respectively. Compared to Fc-pEG II, Fc-pEG I particles exhibited more aggregation. It is likely that the higher amount of ferrocene moieties probably generated higher **π-π** interaction. In this study, we selected Fc-pEG II for further study in order to decrease the particle aggregation.

Ferrocene-grafted pEGCG-gum (Fc-pEG-gum) was synthesized using ferrocene to pEGCG-gum of 0.1:1. The product, Fc-pEG-gum, gave weight percent of ferrocene in the product of 7.43% (Table 3.1, row 3). Fc-pEG-gum was subjected to SEM and TEM

analyses (Figure 3.5C). The spherical-shaped particles with the size of 150±50 nm were observed. The Fc-pEG-gum showed higher aggregation than Fc-pEG II. This may be a result of the higher molecular weight of the gum material.

Table 3.1 Code, weight ratio of FAA to pEGCG (or pEGCG-gum), weight percent of ferrocene in the product and obtained yield of ferrocene-bearing pEGCG and pEGCG-gum particles

Code	FAA:pEGCG (or pEGCG-gum)	Weight percentage of ferrocene in the product (%)	Yield (%)
Fc-pEG I	1:1	19.77	53.8
Fc-pEG II	0.1:1	4.52	62.9
Fc-pEG-gum	0.1:1	7.43	82.4

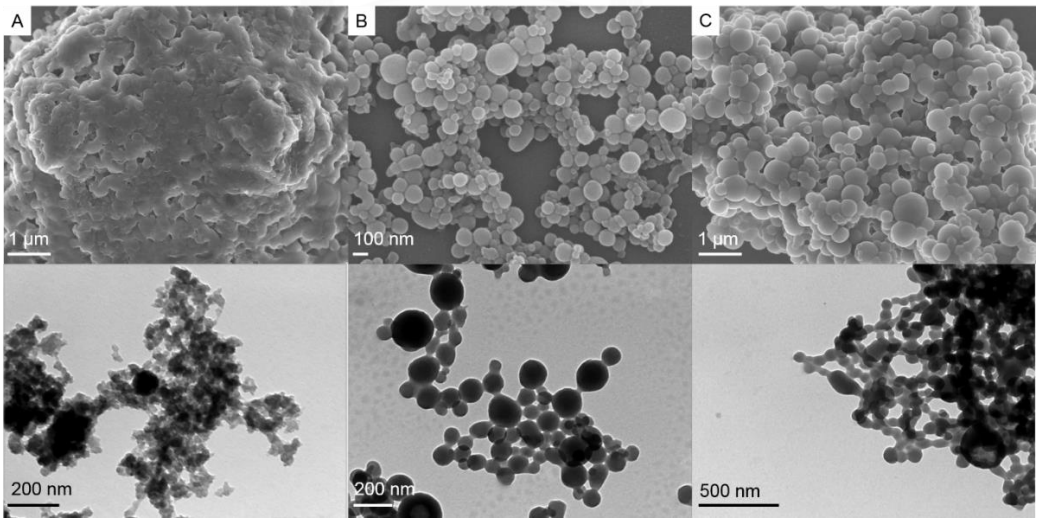

Figure 3.5 SEM (Top) and TEM (Bottom) images of (A) Fc-pEG I, (B) Fc-pEG II and (C) Fc-pEG-gum

The three dry products are black powder. Fc-pEG I, Fc-pEG II and Fc-pEG-gum were all insoluble in hexane, dichloromethane (CH_2Cl_2), chloroform ($CHCl_3$), ethyl acetate (EtOAc), MeOH, ethanol (EtOH), acetone, DMF, dimethyl sulfoxide (DMSO) and deionized water (DI water) as illustrated in Figure 3.6.

Besides Morphological study and solubility of the obtained products, we also investigated the chemical components and thermal property of ferrocene-bearing particles. As mentioned above, Fc-pEG I particles exhibited the most aggregation (Figure 3.5A). Therefore, the lower weight percent of ferrocene particles (Fc-pEG II and Fc-pEG-gum) were selected for further studies.

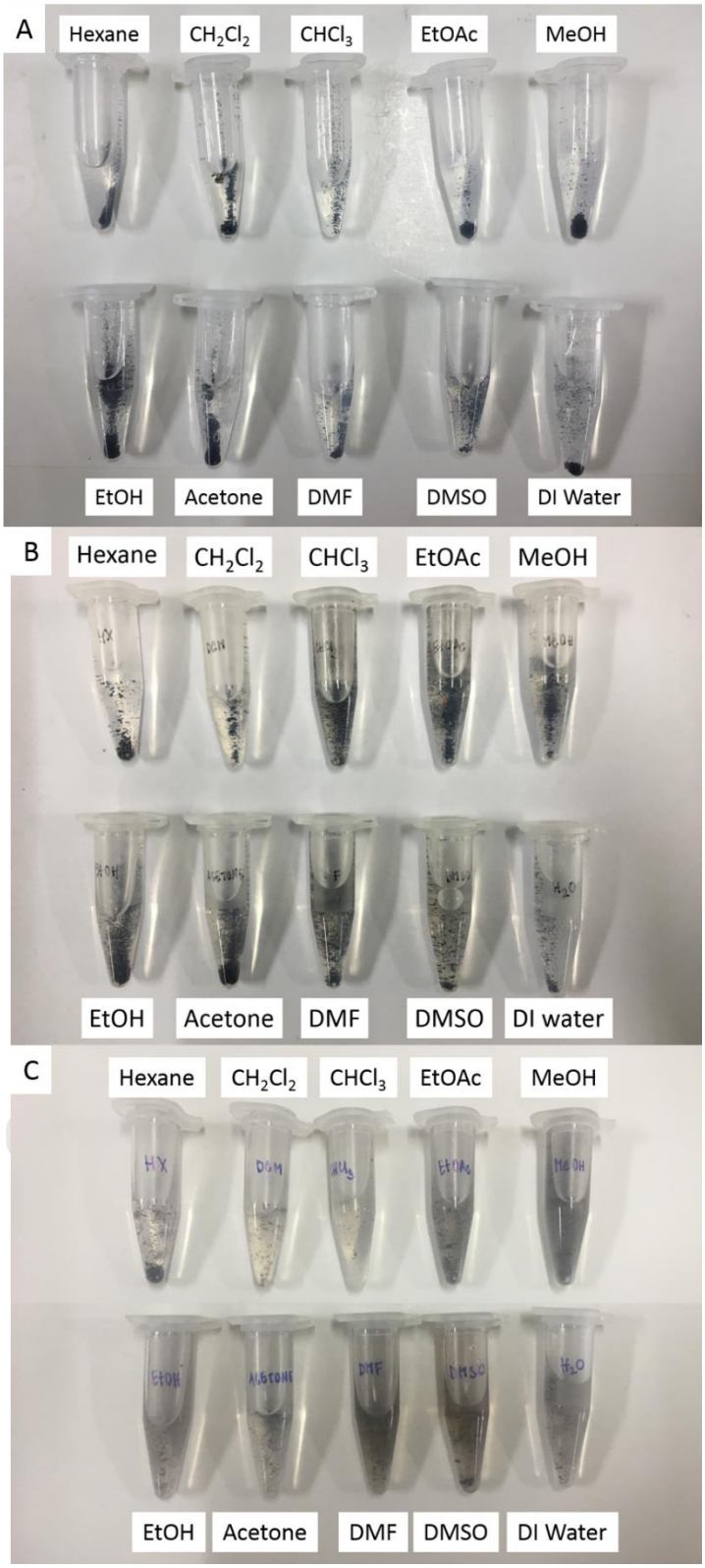

Figure 3.6 Solubility test of (A) Fc-pEG I (B) Fc-pEG II and (C) Fc-pEG-gum in various solvents

To confirm the incorporation of ferrocene into pEGCG and pEGCG-gum, transmission electron microscope coupled with energy dispersive x-ray spectrometer was used (Figure 3.7). The results showed that both Fc-pEG II and Fc-pEG-gum contained carbon and oxygen peaks attributable to pEGCG and pEGCG-gum, and iron peaks attributable to ferrocene moieties. The results confirm the presence of ferrocene in the two particles.

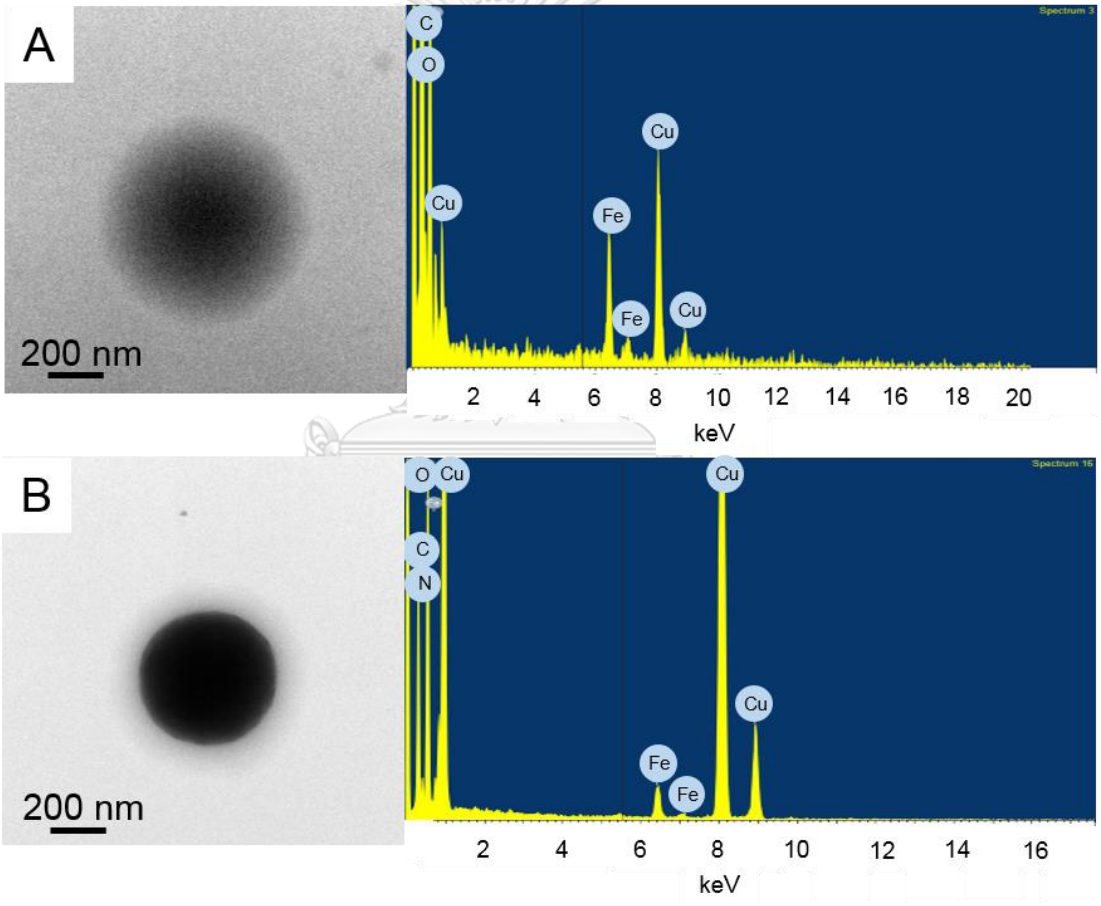

Figure 3.7 TEM (left) and EDX analysis (right) images of (A) Fc-pEG II and (B) Fc-pEG-gum

To confirm the grafting of ferrocene onto pEGCG and EGCG-gum, FTIR spectroscopy was used. FTIR spectra of Fc-pEG II (Figure 3.8) show the vibration bands

at 1037.64 (sp2 C-H in-plane bending), 1106.03 (C=C streching) and 1438.72 cm-1 (C=C streching). The similar peaks were also found in Fc-pEG-gum (1036.21, 1104.04 and 1440.36 cm-1). These are characteristic bands related to cyclopentadiene rings of ferrocene observed in 1000.96, 1105.73 and 1407.98 cm-1 [52, 53]. In addition, the shift of C=O stretching band of FAA from 1705.84 cm-1 to 1709.4 and 1708.9 cm-1 in the Fc-pEG II and Fc-pEG-gum indicates the ester formation, thus corresponding well with our expected incorporation of ferrocene into pEGCG and pEGCG-gum via an ester bond.

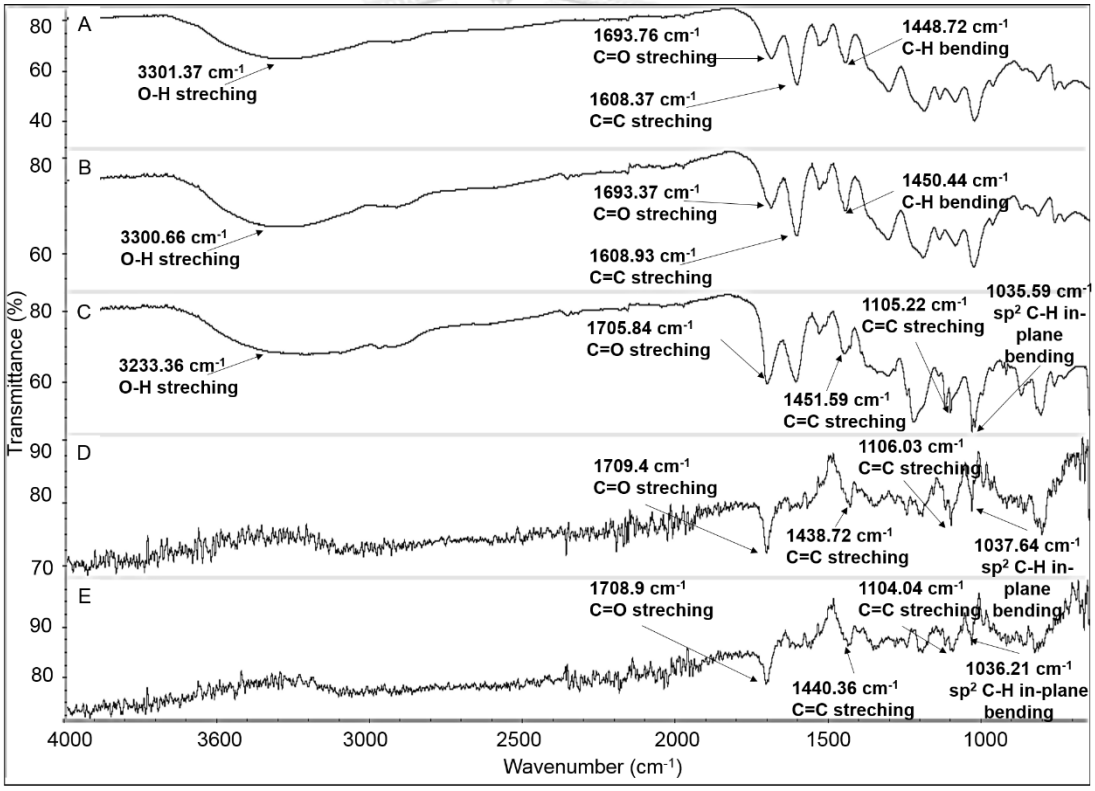

Figure 3.8 FTIR spectra of (A) pEGCG, (B) pEGCG-gum, (C) FAA, (D) Fc-pEG II and (E) Fc-pEG-gum

The functional groups on the surface of ferrocene-bearing pEGCG and pEGCG-gum were evaluated by XPS technique (Figure 3.9). Deconvoluted C1s spectra of Fc-

pEG II showed peaks, indicating C-C and C-H (282.68 eV), aromatic C=C (284.18 eV), epoxy C-O (285.68 eV), carbonyl C=O (286.68 eV) and O=C-O (288.68 eV) [54-56]. Deconvoluted O1s spectra of Fc-pEG II showed peaks at 530.24 and 532.24 eV, corresponding to C=O and O=C-O, respectively [57]. Deconvoluted Fe2p spectra of Fc-pEG II showed peaks at 710.99 and 723.99 eV which are attributed to $Fe2p_{3/2}$ and $Fe2p_{1/2}$ of Fe(II) [58, 59]. The appearance of O=C-O and Fe(II) spectra confirmed the grafting of ferrocene moieties onto pEGCG via ester bond.

Deconvoluted C1s spectra of Fc-pEG-gum showed peaks at 283.23 eV (C-C, C-H), 284.73 eV (aromatic C=C), 286.23 eV (epoxy C-O), 287.23 eV (carbonyl C=O) and 289.23 eV (O=C-O). Deconvoluted O1s spectra of Fc-pEG-gum showed peaks at 531.15 and 534.62 eV, indicating the C=O and O=C-O, respectively. Deconvoluted Fe2p spectra of Fc-pEG-gum showed the peaks at 709.75 and 722.75 eV attributable to $Fe2p_{3/2}$ and $Fe2p_{1/2}$ of Fe(II). Comparing to Fc-pEG II, Fc-pEG-gum showed higher O=C-O, $Fe2p_{3/2}$ and $Fe2p_{1/2}$ of Fe(II) intensity. The results implying higher amount of grafted-ferrocene moieties in Fc-pEG-gum than Fc-pEG II. The results corresponded well with weight percent of ferrocene in the product (7.43% for Fc-pEG-gum and 4.52% for Fc-pEG II). From FTIR and XPS results, we proposed the structure of ferrocene-bearing particles (Fc-pEG and Fc-pEG-gum) as shown in Figure 3.10

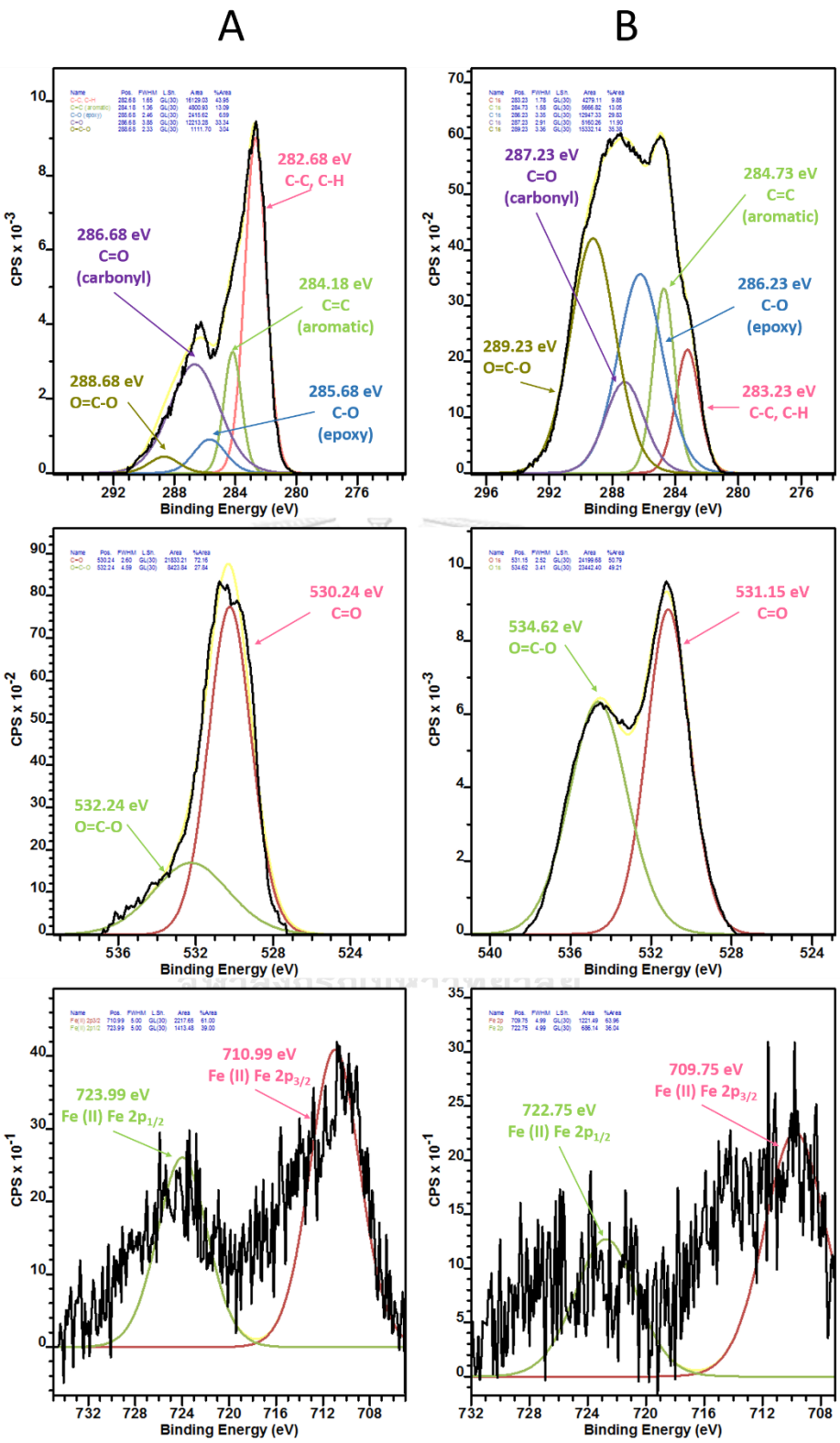

Figure 3.9 Chemical analysis of (A) Fc-pEG II and (B) Fc-pEG-gum by XPS: C1s core-level spectra (top), O1s core-level spectra (middle) and Fe2p core-level spectra (bottom).

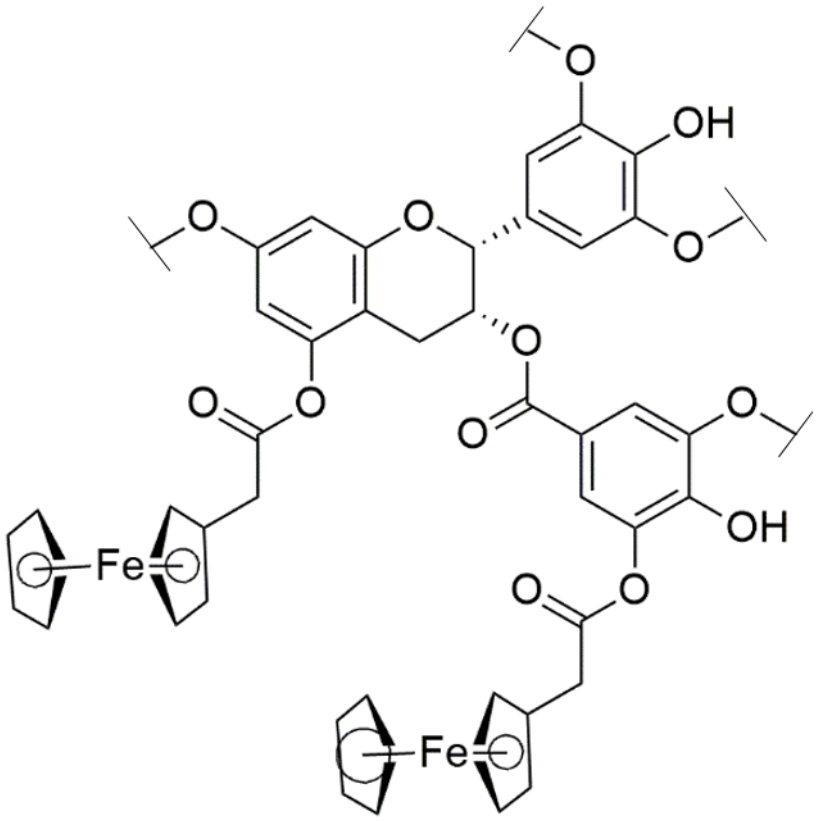

Figure 3.10 Proposed structure of ferrocene-bearing particles

Thermal property of ferrocene-bearing pEGCG and pEGCG-gum was observed by thermal gravimetric analysis technique (Figure 3.11). Thermogram of pEGCG (orange line) showed endothermic peaks at 69 ^{o}C, 246 ^{o}C and 350 ^{o}C that accounted for 8.65%, 30.65% and 24.37% of total mass loss. Compared to pEGCG, Fc-pEG II (purple line) showed 3 endothermic peaks at 60 ^{o}C, 250 ^{o}C and 340 ^{o}C (accounted for 6.47%, 18% and 45.11% of total mass loss). The shift of endothermic peaks upon ferrocene grafting indicates the change of chemical constituents which affect inter/intra molecular bonding.

pEGCG-gum (green line) showed endothermic peaks at 70 ^{o}C, 255 ^{o}C and 370 ^{o}C, accounted for 3.42%, 30.52% and 40.44%. Fc-pEG-gum (blue line) showed endothermic peaks at 55 ^{o}C, 250 ^{o}C and 347 ^{o}C (accounted for 5.9%, 12.72% and 53.24% of total mass loss). All peaks shifted to lower temperature as compared to pEGCG-gum. The peak shifting of Fc-pEG II and Fc-pEG-gum confirms the chemical modification of ferrocene into pEGCG and pEGCG-gum.

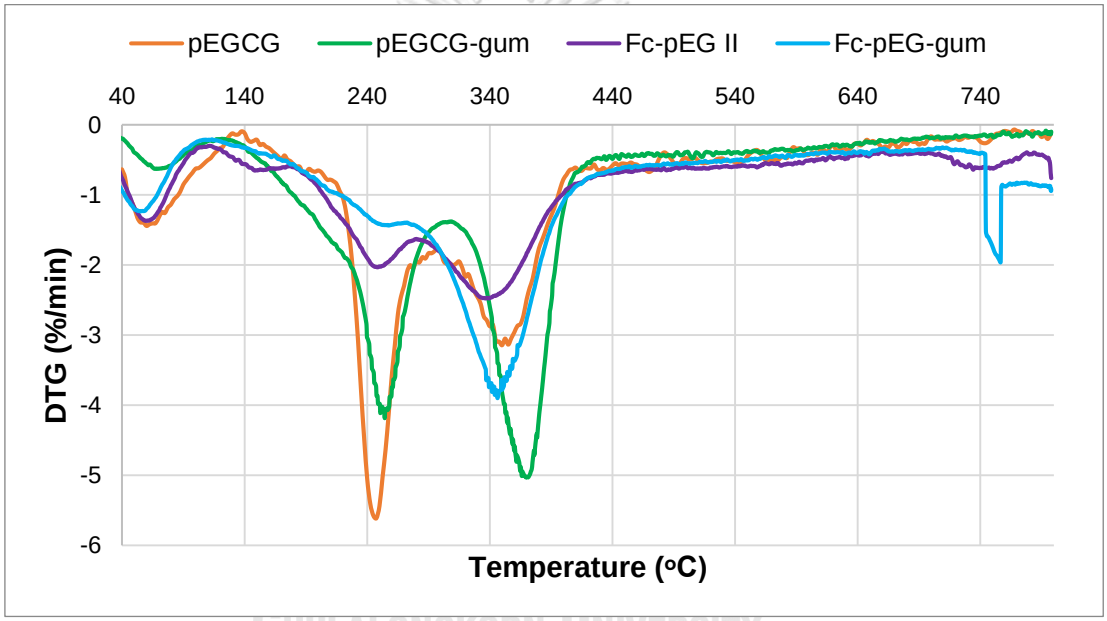

Figure 3.11 TGA thermogram of pEGCG (orange line), pEGCG-gum (green line), Fc-pEG II (purple line) and Fc-pEG-gum (blue line)

3.3 Oxidation-responsive study of Fc-pEG and Fc-EG-gum

Ferrocene can be oxidized by hydrogen peroxide [60, 61]. Ferrocene has been used as oxidation-responsive moiety in various drug delivery systems [48, 49]. In this work, we studied oxidation-responsiveness of ferrocene-bearing particles of Fc-pEG I,

Fc-pEG II and Fc-pEG-gum using hydrogen peroxide as an oxidizing agent. Fc-pEG I changed from black precipitates to light yellow solution upon hydrogen peroxide exposure (1000 mM, 45 min). The same change was observed in Fc-pEG II (1000 mM, 3.5 h) and Fc-pEG-gum (1000 mM, 1.5 h), respectively (Figure 3.12). The yields of oxidation products from the three ferrocene-bearing particles are shown in Table 3.2. As compared to Fc-pEG II (Figure 3.12, middle), Fc-pEG I was oxidized more quickly (Figure 3.12, top). We speculate that the higher weight percent of ferrocene in the particles is the reason behind this observation. In addition, ferrocene-bearing particles made from pEGCG-gum was oxidized more quickly than particles made from pEGCG. The results corresponded well to the weight percent of ferrocene (Table 3.1). The weight percent of ferrocene of Fc-pEG-gum (7.43%) was higher than Fc-pEG II (4.52%). Table 3.3 shows weight percentage of ferrocene incorporated into pEGCG or pEGCG-gum before and after oxidation. Weight percent of ferrocene in Fc-pEG I and Fc-pEG II was 19.77 and 4.52%, respectively. After oxidation, weight percent of ferrocene in oxidized products (oxFc-pEG I and oxFc-pEG II) increased to 46.92 and 37.47%, respectively. The weight percent of ferrocene in Fc-pEG-gum increased from 7.43 to 40.11% upon oxidation. The increase of weight percent of ferrocene in the three ferrocene-bearing particles suggested that not only ferrocene moieties were oxidized but organic components from pEGCG and pEGCG-gum were probably converted into carbon dioxide.

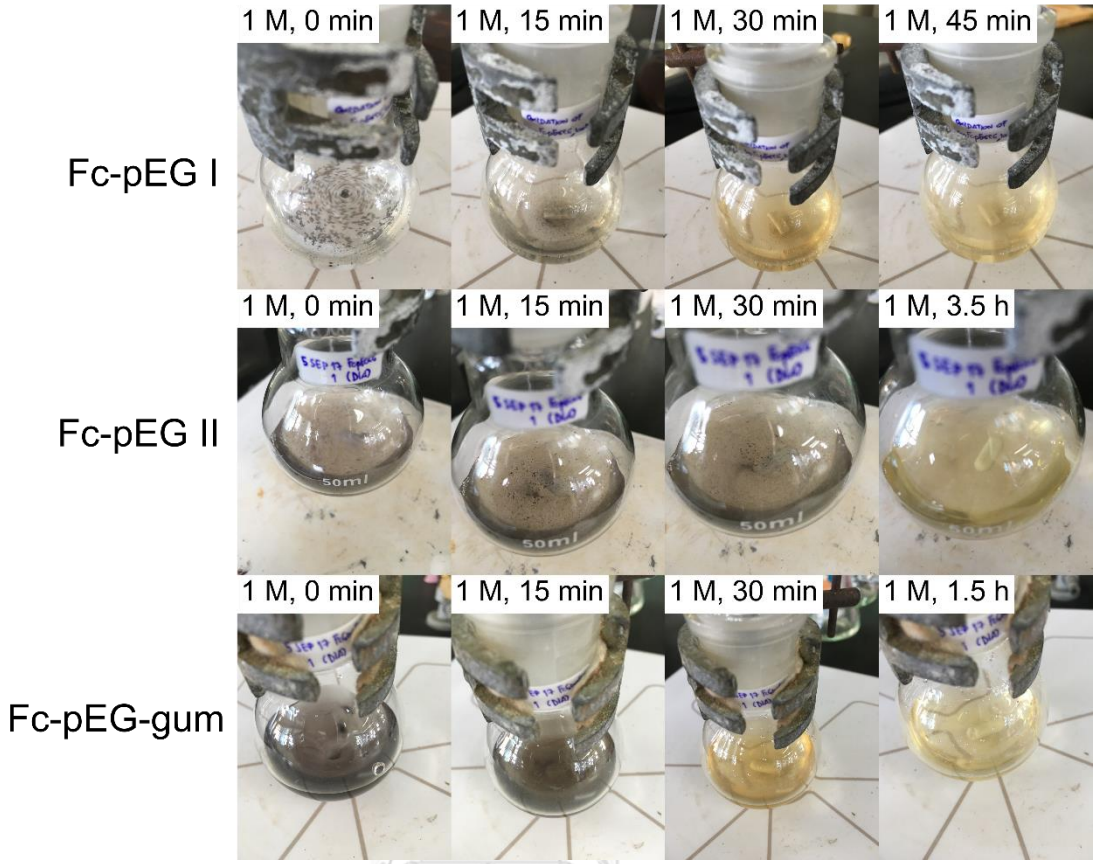

Figure 3.12 Oxidation by hydrogen peroxide of the Fc-pEG I (top), Fc-pEG II (middle) and Fc-pEG-gum (bottom)

Table 3.2 Code and the yield of the oxidation of the three ferrocene-grafted polymerized EGCG materials.

Code	Yield (%)
oxFc-pEG I	39.8
oxFc-pEG II	10.1
oxFc-pEG-gum	3.98

Table 3.3 Weight percentage of ferrocene incorporated in the particles before and after oxidation

Sample	Weight percentage of ferrocene incorporated into the particles (%)
Fc-pEG I	19.77
Fc-pEG II	4.52
Fc-pEG-gum	7.43
oxFc-pEG I	46.92
oxFc-pEG II	37.47
oxFc-pEG-gum	40.11

oxFc-pEG II and oxidized ferrocene-bearing particles made from gum (oxFc-pEG-gum) were subjected to SEM and TEM analyses. The results showed spherical-shaped particles with sizes of 20±5 and 50±20 nm for oxFc-pEG II and oxFc-pEG-gum, respectively (Figure 3.13B and C). The results corresponded well with dynamic light scattering results for oxFc-pEG II and oxFc-pEG-gum of 20.01±0.54 and 55.86±1.23 nm, respectively (Table 3.4). SEM analysis revealed that oxFc-pEG I was spherical with the size of 20±10 nm (Figure 3.13A). Dynamic light scattering results of oxFc-pEG I showed

bigger size compared to SEM image. The fact that Fc-pEG I aggregates well correspond to its low zeta-potential values (Table 3.4).

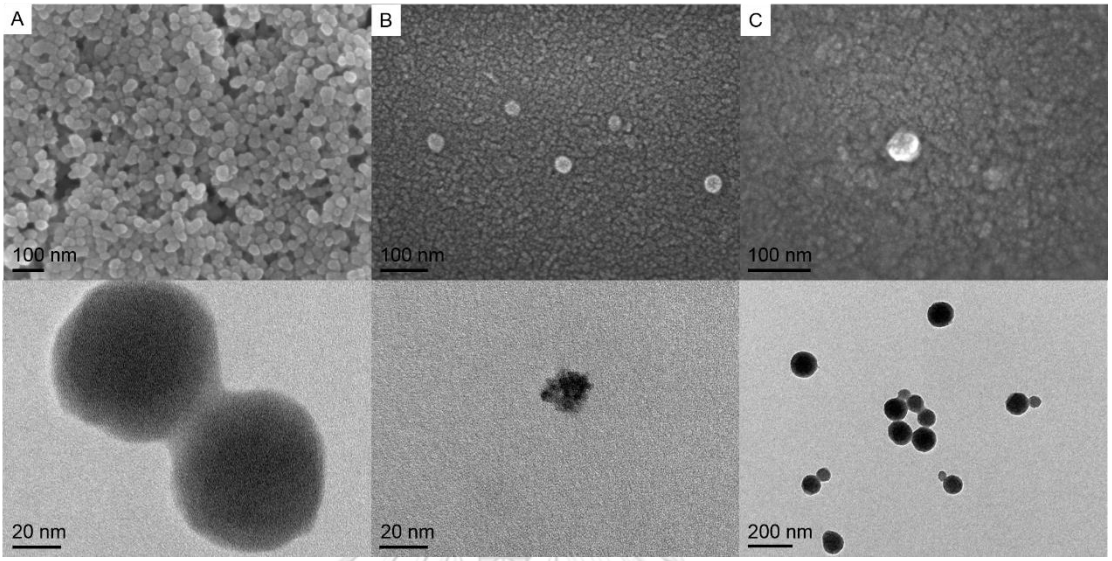

Figure 3.13 SEM (Top) and TEM (Bottom) images of (A) oxFc-pEG I, (B) oxFc-pEG II and (C) oxFc-pEG-gum

Table 3.4 Particles sizes and zeta-potential values of the three oxidized Ferrocene-bearing particles

Code	Particle size (nm)		Zeta-potential (mV)
	SEM	DLS	
oxFc-pEG I	20±10	67.60±6.36	-15.2
oxFc-pEG II	20±5	20.01±0.54	-30.1
oxFc-pEG-Gum	50±20	55.86±1.23	-18.9

Chemical composition after oxidation was also investigated using FTIR spectroscopy. Compared to Fc-pEG II (Figure 3.14), oxFc-pEG II also showed the vibration bands around 1030-1430 cm^{-1}. The appearance of vibration bands around 1030-1430 cm^{-1} was observed in Fc-pEG-gum (characteristic bands of cyclopentadiene rings of ferrocene at 1000.96, 1105.73 and 1407.98 cm^{-1}, respectively [52, 53]). Moreover, the C=O ester bond stretching band was also observed in oxFc-pEG II and oxFc-pEG-gum at 1709.7 and 1708.28 cm^{-1}, respectively.

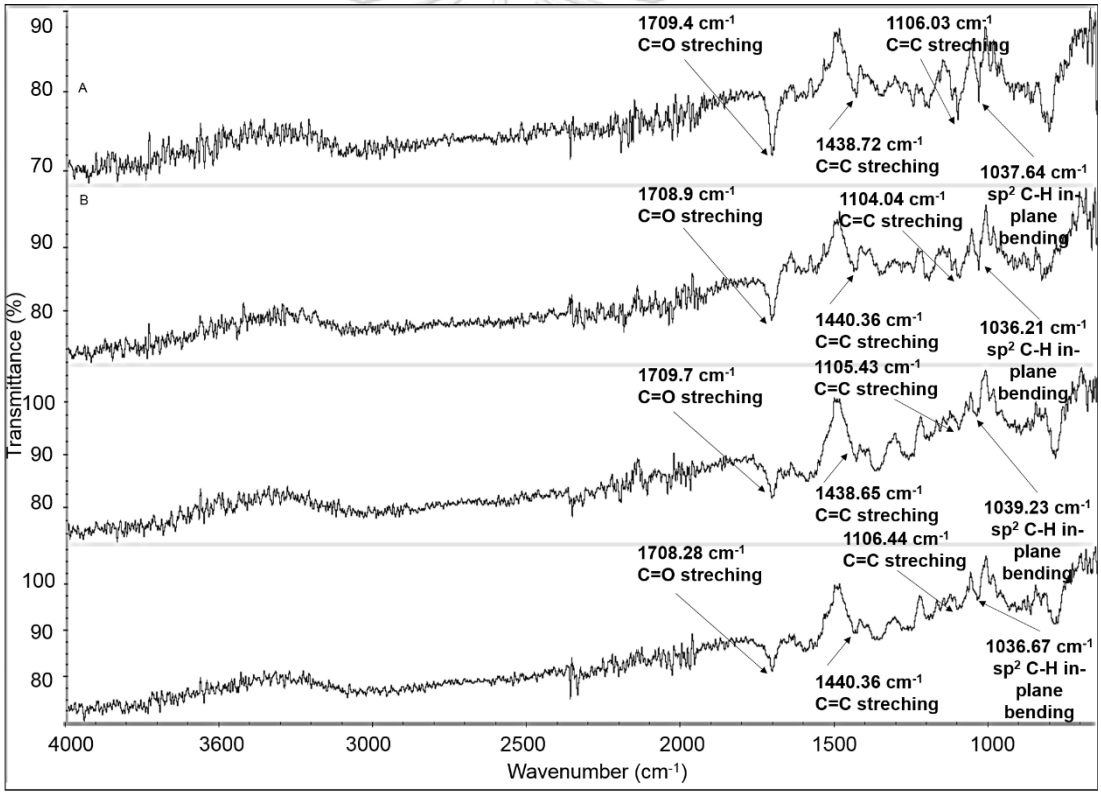

Figure 3.14 FTIR spectra of (A) Fc-pEG II, (B) Fc-pEG-gum, (C) oxFc-pEG II and (D) oxFc-pEG-gum

The XPS spectra were used to determine functional groups on the surface of Fc-pEG II and Fc-pEG-gum after being oxidized (Figure 3.15). Deconvoluted C1s spectra

of oxFc-pEG II showed 5 main peaks observed in the original materials (Figure 3.9). The results showed C-C and C-H (283.44 eV), aromatic C=C (284.94 eV), epoxy C-O (286.44 eV), carbonyl C=O (287.44 eV) and O=C-O (289.44 eV) [54-56]. Apart from the 5 peaks, oxFc-pEGCG showed an extra peak at 292.28 eV, a shake-up satellite peak which corresponds to **π**-**π*** satellite of the extended delocalized electrons [62, 63]. It suggested that oxidation induced further electron delocalization. Deconvoluted O1s spectra oxFc-pEG II revealed 2 peaks at 530.05 and 532.46 eV, corresponding to C=O and O=C-O, respectively [57]. Deconvoluted Fe2p spectra of oxFc-pEG II showed 2 important peaks at 711.26 and 723.26 eV, corresponding to $Fe2p_{3/2}$ and $Fe2p_{1/2}$ of Fe(III) [58, 64]. It implied that ferrocene moieties turned to ferrocenium ion upon oxidation. In addition, oxFc-pEG II showed another peak at 708.26 eV which is $Fe2p_{3/2}$ of Fe(II) [58, 59]. The results indicated that ferrocene moieties in Fc-pEG II wasn't totally oxidized.

Deconvoluted C1s spectra of oxFc-pEG-gum showed 5 main peaks observed in Fc-pEG-gum (Figure 3.9B). The results showed C-C and C-H (283.07 eV), aromatic C=C (284.57 eV), epoxy C-O (286.07 eV), carbonyl C=O (287.07 eV) and O=C-O (289.57 eV) [54-56]. Deconvoluted O1s spectra oxFc-pEG-gum revealed 2 peaks at 530.40 and 532.64 eV, corresponding to C=O and O=C-O, respectively [57]. oxFc-EG-gum showed a reduction of C=O intensity and the increase of O=C-O intensity, as compared to Fc-EG-gum. The results indicated that carbonyl groups of Fc-pEG-gum turned to O=C-O

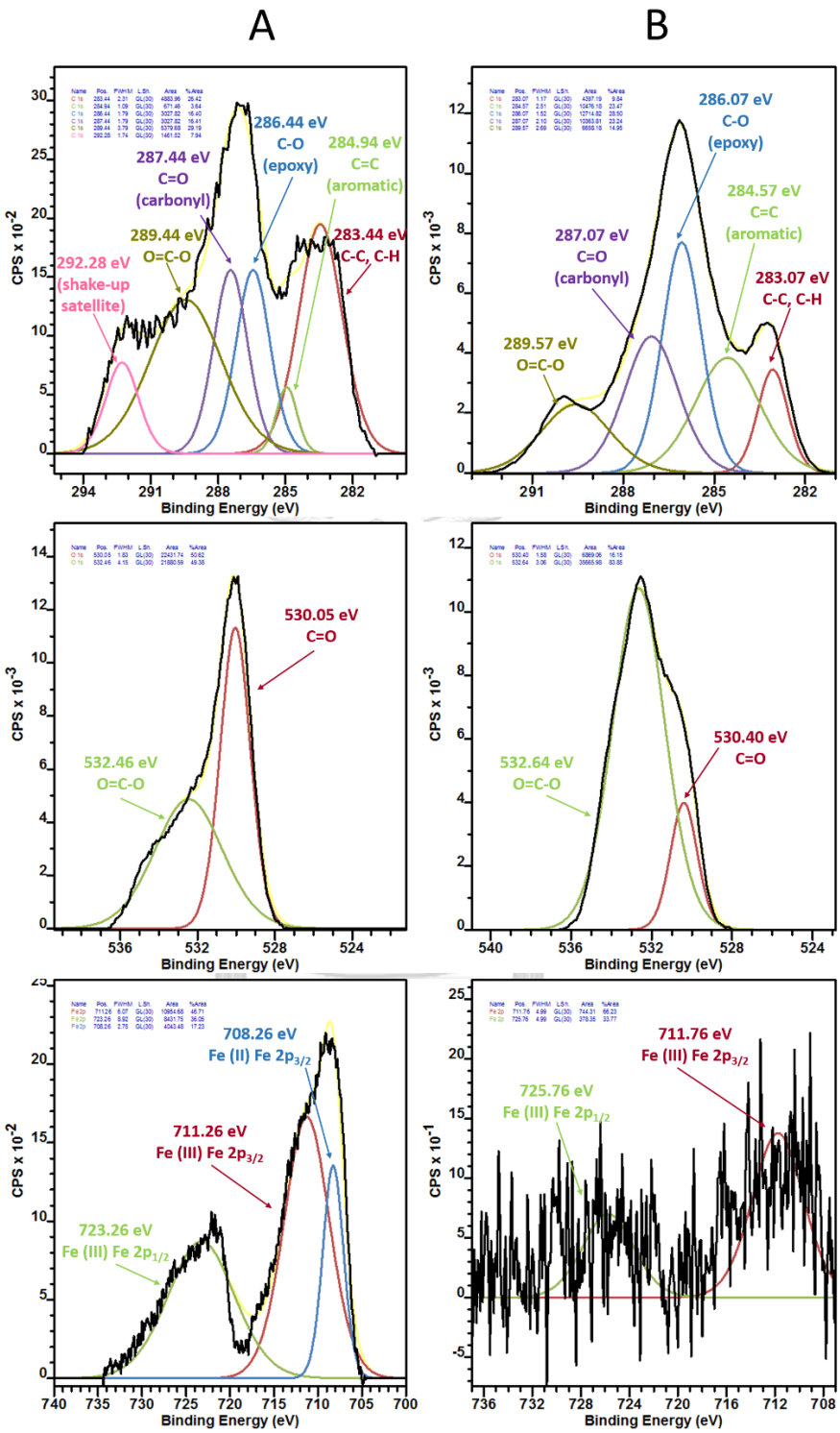

Figure 3.15 Chemical analysis of (A) oxFc-pEG II and (B) oxFc-pEG-gum by XPS: C1s core-level spectra (top), O1s core-level spectra (middle) and Fe2p core-level spectra (bottom)

groups upon oxidation. Deconvoluted Fc2p spectra of oxFc-pEG-gum showed 2 peaks at 711.76 and 725.76 eV, corresponding to $Fe2p_{3/2}$ and $Fe2p_{1/2}$ of Fe(III) [58, 64].

Thermal property of oxFc-pEG II and oxFc-pEG-gum was investigated by TGA (Figure 3.16). oxFc-pEG II (red line) showed peaks at 110 ^{o}C, 190 ^{o}C and 460 ^{o}C (accounted for 6.18%, 65.17% and 40.47% of the total mass loss). The peak at 336.4 ^{o}C observed in Fc-pEG II (purple line) could not be observed in the oxidized product. A new peak at 460 ^{o}C appeared in the oxidized product. The results implied that oxidation of ferrocene-bearing pEGCG probably induce the reorganization of chemical interactions within the particles in each a way that makes a certain portion of the particles more heat stable (degrades at higher temperature). Thermogram of oxFc-pEG-gum (yellow line) showed 3 peaks at 95 ^{o}C, 195 ^{o}C and 310 ^{o}C (accounted for 9.5%, 55.48% and 39.29% of the total mass loss). Compared to Fc-pEG-gum (blue line), the shifted of endothermic peaks after oxidation was observed, thus indicating that oxidation produced a functional change that affected thermal property of the materials.

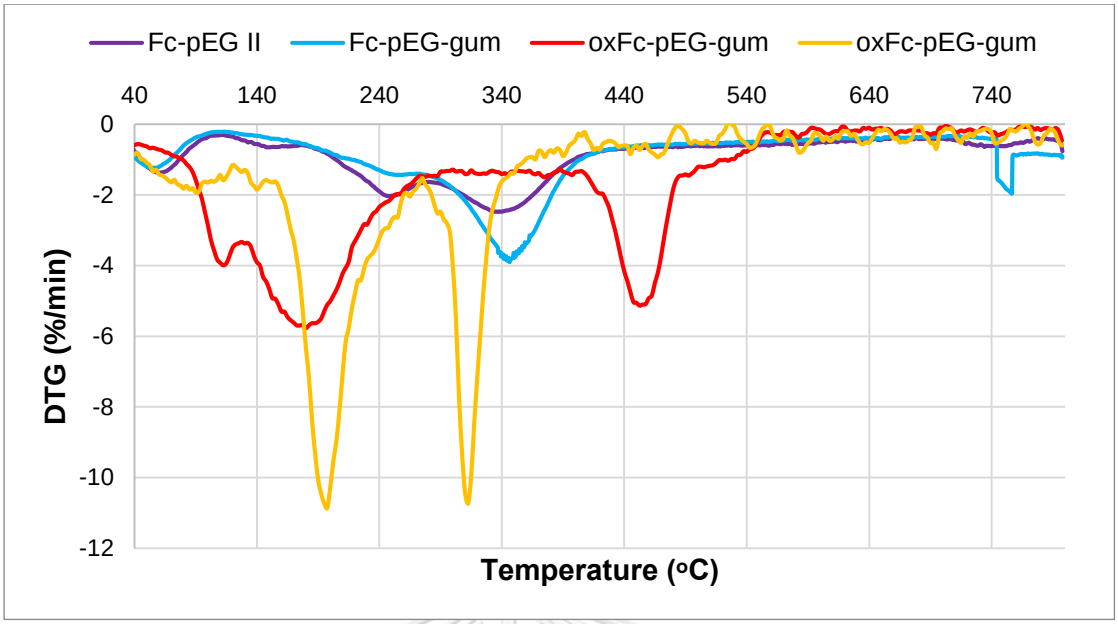

Figure 3.16 TGA thermogram of Fc-pEG II (purple line), Fc-pEG-gum (blue line), oxFc-pEG II (red line) and oxFc-pEG-gum (yellow line)

To evaluate the anti-cancer activity of the oxidized particles, we used MTT assay to determine the cell viability. The oxFc-pEG I, oxFc-pEG II and oxFC-pEG-gum were tested against HepG2 liver cancer cells using EGCG, pEGCG, EGCG-gum, and paclitaxel (PTX) as controls (Figure 3.17). The results showed that oxFc-pEG-gum (Figure 3.17, yellow line) possed about 30% growth inhibition of cancer cells at 100 μg/mL. oxFc-pEG-gum exhibited less cancer cell growth inhibition when compared to that of the controls (EGCG, pEGCG, pEGCG-gum and PTX). The anti-cancer activity of pEGCG-gum was tested using pEGCG-gum in DMSO, whereas that of the oxFc-pEG-gum was tested in water. We expect that if the amount of ferrocene moieties on the polymers is reduced, more anti-cancer activity might be obtained. This work will be our future work.

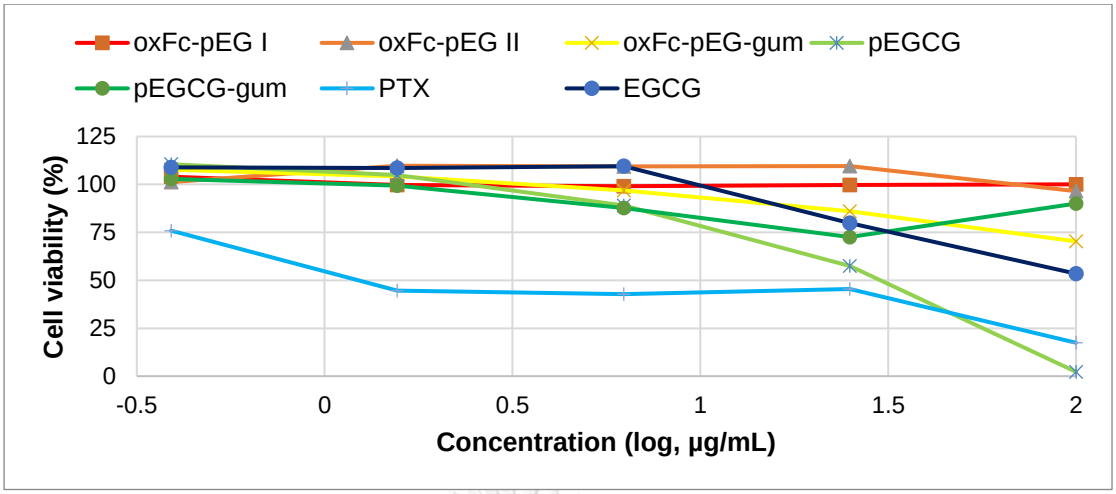

Figure 3.17 Cell viability of HepG2 cell with oxFc-pEG I (red line), oxFc-pEG II (orange line), oxFc-pEG-gum (yellow line), pEGCG (light green line), pEGCG-gum (dark green line), PTX (blue line) and EGCG (purple line)

CHAPTER IV

CONCLUSION

Ferrocene moieties were grafted onto pEGCG and pEGCG-gum, the polymerized EGCG particles and the polymerized EGCG gum, respectively. Three weight percents of ferrocene in the products, 19.77, 4.52 and 7.43% (depicted as Fc-pEG I, Fc-pEG II and Fc-pEG-gum) were prepared. To study effect of amount of ferrocene using Fc-pEG I and Fc-pEG II which boths were synthesized from pEGCG and effect of starting material (pEGCG and pEGCG-gum) using Fc-pEG II and Fc-pEG-gum which the latter was synthesized from pEGCG-gum. The yield of ferrocene-bearing products, 19.77, 4.52 and 7.43% were obtained in 53.8%, 62.9% and 82.8%, respectively. The morphology of three ferrocene-bearing products was spherical-shaped with various particle size. The size of Fc-pEG I was around 200±20 nm. Fc-pEG II was 100±20 and 200±20 nm. Fc-pEG-gum was 100±50 nm to 1000±80 nm. TEM-EDX spectra of ferrocene-bearing particles revealed the incorporation of iron in particles. FTIR and XPS techniques indicated the successful grafting of ferrocene onto pEGCG and EGCG-gum through the appearance of vibrational bands around 1000-1400 cm^{-1}, indicating cyclopentadiene characteristic peaks of ferrocene and the shifting of C=O stretching from 1705.84 cm^{-1} (observed in ferroceneacetic acid) to around 1708 cm^{-1} which are attributed to ester bond. Moreover, deconvoluted Fe2p spectra revealed the peaks at 710 and 723 eV, corresponding to Fe(II) binding energy of ferrocene moieties. Oxidation-responsiveness

of three ferrocene-bearing particles were tested by hydrogen peroxide. All ferrocene-bearing particles were changed from water-insoluble black precipitates to light yellow solution. However, FTIR, XPS, TGA and ICP-OES results of three oxidized ferrocene-bearing particles revealed that not only ferrocene moieties were oxidized but also organic components from pEGCG and pEGCG-gum were affected. The anti-cancer activity of three oxidized ferrocene-bearing particles was evaluated using MTT assay. The results showed that the oxidized particles of Fc-pEG I and Fc-pEG II exhibited no growth inhibition of HepG2 liver cancer cells (IC_{50} > 100 μg/mL). Fc-pEG-gum particles showed 30% growth inhibition of cancer cells at 100 μg/mL. However, Fc-pEG-gum exhibited less cancer cell growth inhibition than controls (PTX, EGCG, pEGCG and pEGCG-gum), we hope that the oxidation with lower concentration (below 1000 mM) and reduction the amount of ferrocene in particles could alter the anti-cancer activity of oxidized ferrocene-bearing particle.

REFERENCES

1. Wilailak, S. and N. Lertchaipattanakul, *The epidemiologic status of gynecologic cancer in Thailand.* Journal of gynecologic oncology, 2016. **27**(6).

2. Varpe, P., et al., *Quality of life after surgery for rectal cancer with special reference to pelvic floor dysfunction.* Colorectal Disease, 2011. **13**(4): p. 399-405.

3. Inoue, T., H. Shiomi, and R.-J. Oh, *Stereotactic body radiotherapy for Stage I lung cancer with chronic obstructive pulmonary disease: special reference to survival and radiation-induced pneumonitis.* Journal of radiation research, 2015. **56**(4): p. 727-734.

4. Kaufmann, S.H. and W.C. Earnshaw, *Induction of apoptosis by cancer chemotherapy.* Experimental cell research, 2000. **256**(1): p. 42-49.

5. Eastman, A., *Characterization of the adducts produced in DNA by cis-diamminedichloroplatinum (II) and cis-dichloro (ethylenediamine) platinum (II).* Biochemistry, 1983. **22**(16): p. 3927-3933.

6. Longley, D.B., D.P. Harkin, and P.G. Johnston, *5-fluorouracil: mechanisms of action and clinical strategies.* Nature Reviews Cancer, 2003. **3**(5): p. 330-338.

7. Jordan, M.A. and L. Wilson, *Microtubules as a target for anticancer drugs.* Nature Reviews Cancer, 2004. **4**(4): p. 253-265.

8. Dong, X. and R.J. Mumper, *Nanomedicinal strategies to treat multidrug-resistant tumors: current progress.* Nanomedicine, 2010. **5**(4): p. 597-615.

9. Hail, N., et al., *Cancer chemoprevention: a radical perspective.* Free Radical Biology and Medicine, 2008. **45**(2): p. 97-110.

10. Zaffaroni, A., *Drug-delivery system*. 1974, Google Patents.

11. Schmaljohann, D., *Thermo-and pH-responsive polymers in drug delivery.* Advanced drug delivery reviews, 2006. **58**(15): p. 1655-1670.

12. Zong, W., et al., *Polydopamine-coated liposomes as pH-sensitive anticancer drug carriers.* Journal of microencapsulation, 2016. **33**(3): p. 257-262.

13. Luo, Z., et al., *Redox-Responsive Molecular Nanoreservoirs for Controlled Intracellular Anticancer Drug Delivery Based on Magnetic Nanoparticles.* Advanced Materials, 2012. **24**(3): p. 431-435.

14. Chang, Y.T., et al., *Near-Infrared Light-Responsive Intracellular Drug and siRNA Release Using Au Nanoensembles with Oligonucleotide-Capped Silica Shell.* Advanced Materials, 2012. **24**(25): p. 3309-3314.

15. Karimi, M., et al., *Temperature-responsive smart nanocarriers for delivery of therapeutic agents: applications and recent advances.* ACS applied materials & interfaces, 2016. **8**(33): p. 21107.

16. Hayashi, K., et al., *High-frequency, magnetic-field-responsive drug release from magnetic nanoparticle/organic hybrid based on hyperthermic effect.* ACS applied materials & interfaces, 2010. **2**(7): p. 1903-1911.

17. Koushik, O., et al., *Nano drug delivery systems to overcome cancer drug resistance-a review.* J Nanomed Nanotechnol, 2016. **7**(378): p. 2.

18. Samuelson, G., *Drugs of natural origin: a textbook of pharmacognosy*. 1999, Taylor & Francis Group.

19. Harvey, A.L., *Natural products in drug discovery.* Drug discovery today, 2008. **13**(19): p. 894-901.

20. Mitchell, D.C., et al., *Beverage caffeine intakes in the US.* Food and Chemical Toxicology, 2014. **63**: p. 136-142.

21. Witherup, K.M., et al., *Taxus spp. needles contain amounts of taxol comparable to the bark of Taxus brevifolia: analysis and isolation.* Journal of Natural Products, 1990. **53**(5): p. 1249-1255.

22. Fischer, J. and C. Robin Ganellin, *Analogue-based Drug Discovery.* Chemistry International, 2010. **32**(4): p. 12.

23. Graham, H.N., *Green tea composition, consumption, and polyphenol chemistry.* Preventive medicine, 1992. **21**(3): p. 334-350.

24. Balentine, D.A., S.A. Wiseman, and L.C. Bouwens, *The chemistry of tea flavonoids.* Critical Reviews in Food Science & Nutrition, 1997. **37**(8): p. 693-704.

25. Miyoshi, N., et al., *Green tea catechins for well-being and therapy: prospects and opportunities.* Botanics: Targets Therapy, 2015. **5**: p. 85-96.

26. Shi-chang, L., C. Chi-Kun, and H. Hwa-chung, *THE COMPARATIVE STUDIES ON QUANTITATIVE DETERMINATION OF TEA CATECHU BY PAPER CHROMATOGRAPHY.* Acta Horticulturae Sinica, 1963. **4**: p. 011.

27. Bhatia, I. and M.R. Ullah, *Polyphenols of tea. IV.—Qualitative and quantitative study of the polyphenols of different organs and some cultivated varieties of tea plant.* Journal of the Science of Food and Agriculture, 1968. **19**(9): p. 535-542.

28. Jin, P., et al., *Epigallocatechin-3-gallate (EGCG) as a pro-osteogenic agent to enhance osteogenic differentiation of mesenchymal stem cells from human bone marrow: an in vitro study.* Cell and tissue research, 2014. **356**(2): p. 381-390.

29. Du, X., et al., *Epigallocatechin-3-gallate (EGCG) enhances the therapeutic activity of a dental adhesive.* Journal of dentistry, 2012. **40**(6): p. 485-492.

30. Cavet, M.E., et al., *Anti-inflammatory and anti-oxidative effects of the green tea polyphenol epigallocatechin gallate in human corneal epithelial cells.* Molecular vision, 2011. **17**: p. 533.

31. Naasani, I., H. Seimiya, and T. Tsuruo, *Telomerase inhibition, telomere shortening, and senescence of cancer cells by tea catechins.* Biochemical and biophysical research communications, 1998. **249**(2): p. 391-396.

32. Hibasami, H., et al., *Induction of apoptosis in human stomach cancer cells by green tea catechins.* Oncology reports, 1998. **5**(2): p. 527-536.

33. Ishino, A., et al., *Effect of anticancer drugs, metals and antioxidants on cytotoxic activity of epigallocatechin gallate.* Anticancer research, 1999. **19**(5B): p. 4343-4348.

34. Wang, Y.-C. and U. Bachrach, *The specific anti-cancer activity of green tea (–)-epigallocatechin-3-gallate (EGCG).* Amino acids, 2002. **22**(2): p. 131-143.

35. Du, G.-J., et al., *Epigallocatechin Gallate (EGCG) is the most effective cancer chemopreventive polyphenol in green tea.* Nutrients, 2012. **4**(11): p. 1679-1691.

36. Kwak, T.W., et al., *anticancer activities of epigallocatechin-3-gallate against cholangiocarcinoma cells.* OncoTargets and therapy, 2017. **10**: p. 137.

37. Subramanian, N., et al., *Role of polyphenol oxidase and peroxidase in the generation of black tea theaflavins.* Journal of agricultural and food chemistry, 1999. **47**(7): p. 2571-2578.

38. Bhattacharya, U., S. Mukhopadhyay, and A.K. Giri, *Comparative antimutagenic and anticancer activity of three fractions of black tea polyphenols thearubigins.* Nutrition and cancer, 2011. **63**(7): p. 1122-1132.

39. Pan, M.-H., et al., *Induction of apoptosis by the oolong tea polyphenol theasinensin A through cytochrome c release and activation of caspase-9 and caspase-3 in human U937 cells.* Journal of agricultural and food chemistry, 2000. **48**(12): p. 6337-6346.

40. Babich, H., et al., *Theaflavin-3-Gallate and Theaflavin-3′-Gallate, Polyphenols in Black Tea with Prooxidant Properties.* Basic & clinical pharmacology & toxicology, 2008. **103**(1): p. 66-74.

41. Chung, J.E., et al., *Self-assembled micellar nanocomplexes comprising green tea catechin derivatives and protein drugs for cancer therapy.* Nature nanotechnology, 2014. **9**(11): p. 907-912.

42. Liao, B., et al., *(−)-Epigallocatechin gallate (EGCG)-nanoethosomes as a transdermal delivery system for docetaxel to treat implanted human melanoma cell tumors in mice.* International journal of pharmaceutics, 2016. **512**(1): p. 22-31.

43. Pukfukdee, P., *Fabrication of particles from tea polyphenol extract for anticancer activity*, in *Chemistry*. 2016, Chulalongkorn university. p. 94.

44. Togni, A., *Ferrocenes: homogeneous catalysis, organic synthesis, materials science*. 2008: John Wiley & Sons.

45. Pauson, P.L., *Ferrocene—how it all began.* Journal of Organometallic Chemistry, 2001. **637**: p. 3-6.

46. Housecroft, C.E. and A.G. Sharpe, *Inorganic Chemistry*. 2012: Pearson.

47. Yang, E.S., M.-S. Chan, and A.C. Wahl, *Electron exchange between ferrocene and ferrocenium ion. Effects of solvent and of ring substitution on the rate.* The Journal of Physical Chemistry, 1980. **84**(23): p. 3094-3099.

48. Liu, L., et al., *Self-assembly and disassembly of a redox-responsive ferrocene-containing amphiphilic block copolymer for controlled release.* Polymer Chemistry, 2015. **6**(10): p. 1817-1829.

49. Noyhouzer, T., et al., *Ferrocene-Modified Phospholipid: An Innovative Precursor for Redox-Triggered Drug Delivery Vesicles Selective to Cancer Cells.* Langmuir, 2016. **32**(17): p. 4169-4178.

50. Seemork, J., et al., *Penetration of Oxidized Carbon Nanospheres through Lipid Bilayer Membrane: Comparison to Graphene Oxide and Oxidized Carbon Nanotubes, and Effects of pH and Membrane Composition.* ACS applied materials & interfaces, 2016. **8**(36): p. 23549-23557.

51. Lirdprapamongkol, K., et al., *Vanillin suppresses metastatic potential of human cancer cells through PI3K inhibition and decreases angiogenesis in vivo.* Journal of Agricultural and Food Chemistry, 2009. **57**(8): p. 3055-3063.

52. Willis, J., et al., *An infrared and Raman study of 1, 1′-disubstituted ferrocene compounds.* Spectrochimica Acta Part A: Molecular Spectroscopy, 1968. **24**(10): p. 1561-1572.

53. Lokshin, B., V. Aleksanian, and E. Rusach, *On the vibrational assignments of ferrocene, ruthenocene and osmocene.* Journal of Organometallic Chemistry, 1975. **86**(2): p. 253-256.

54. Stankovich, S., et al., *Synthesis of graphene-based nanosheets via chemical reduction of exfoliated graphite oxide.* carbon, 2007. **45**(7): p. 1558-1565.

55. Wang, Y., Z. Shi, and J. Yin, *Facile synthesis of soluble graphene via a green reduction of graphene oxide in tea solution and its biocomposites.* ACS applied materials & interfaces, 2011. **3**(4): p. 1127-1133.

56. Abdullah, M., R. Zakaria, and S. Zein, *Green tea polyphenol–reduced graphene oxide: derivatisation, reduction efficiency, reduction mechanism and cytotoxicity.* RSC Advances, 2014. **4**(65): p. 34510-34518.

57. Cai, H.-m., et al., *X-ray photoelectron spectroscopy surface analysis of fluoride stress in tea (Camellia sinensis (L.) O. Kuntze) leaves.* Journal of Fluorine Chemistry, 2014. **158**: p. 11-15.

58. Biesinger, M.C., et al., *Resolving surface chemical states in XPS analysis of first row transition metals, oxides and hydroxides: Cr, Mn, Fe, Co and Ni.* Applied Surface Science, 2011. **257**(7): p. 2717-2730.

59. Lin, K.Y.A., J.T. Lin, and A.P. Jochems, *Oxidation of amaranth dye by persulfate and peroxymonosulfate activated by ferrocene.* Journal of Chemical Technology and Biotechnology, 2017. **92**(1): p. 163-172.

60. Lubach, J. and W. Drenth, *Enolization and oxidation: II. Oxidation of ferrocene by molecular oxygen and hydrogen peroxide in acidic media.* Recueil des Travaux Chimiques des Pays-Bas, 1973. **92**(6): p. 586-592.

61. Fomin, F. and K. Zaitseva, *Mechanism of the oxidation of ferrocene and its derivatives with hydrogen peroxide: A new effect.* Russian Journal of Physical Chemistry A, 2014. **88**(3): p. 466-470.

62. Beamson, G. and D. Briggs, *High resolution XPS of organic polymers*. 1992: Wiley.

63. Chehimi, M.M., *Aryl diazonium salts: new coupling agents and surface science*. 2012: John Wiley & Sons.

64. WP, W., et al., *XPS and magnetic properties of CoFe2O4 nanoparticles synthesized by a polyacrylamide gel route.* Materials Transactions, 2012. **53**(9): p. 1586-1589.

APPENDIX

1. Calculation of percent yield of pEGCG and EGCG-gum

$$\text{Yield (\%)} = \frac{\text{weight of pEGCG (orp EGCG-gum)}}{\text{weight of EGCG}} \times 100 \quad \text{(Eq. 1)}$$

pEGCG

$$\text{Yield (\%)} = \frac{0.0221\ \text{g}}{0.54\ \text{g}} \times 100$$

Yield (%) = 4.1 %

pEGCG-gum

$$\text{Yield (\%)} = \frac{0.0308\ \text{g}}{0.54\ \text{g}} \times 100$$

Yield (%) = 5.7 %

2. Calculation of percent yield of Fc-pEG and Fc-pEG-gum

$$\text{Yield (\%)} = \frac{\text{weight of Fc-pEG (or Fc-pEG-gum)}}{\text{weight of pEGCG (or pEGCG-gum) + weight of used FAA}} \times 100 \quad \text{(Eq. 2)}$$

Fc-pEG I

$$\text{Yield (\%)} = \frac{59.2\ \text{mg}}{100\ \text{mg} + 10\ \text{mg}} \times 100$$

Yield (%) = 53.8 %

Fc-pEG II

$$\text{Yield (\%)} = \frac{12.6\ \text{mg}}{10\ \text{mg} + 10\ \text{mg}} \times 100$$

Yield (%) = 62.9 %

Fc-pEG-gum

$$\text{Yield (\%)} = \frac{16.5\ \text{mg}}{10\ \text{mg} + 10\ \text{mg}} \times 100$$

Yield (%) = 82.4 %

3. Calculation of percent yield of oxFc-pEG and oxFc-pEG-gum

$$\text{Yield (\%)} = \frac{\text{weight of oxFc-pEG (or oxFc-pEG-gum)}}{\text{weight of Fc-pEG (or Fc-pEG-gum)}} \times 100 \qquad \text{(Eq. 3)}$$

oxFc-pEG I

$$\text{Yield (\%)} = \frac{3.98\ \text{mg}}{10\ \text{mg}} \times 100$$

Yield (%) = 39.8 %

oxFc-pEG II

$$\text{Yield (\%)} = \frac{1.26\ \text{mg}}{10\ \text{mg}} \times 100$$

Yield (%) = 10.1 %

oxFc-pEG-gum

$$\text{Yield (\%)} = \frac{0.39\ \text{mg}}{10\ \text{mg}} \times 100$$

Yield (%) = 3.98 %

4. Thermal properties

Thermatogram of pEGCG

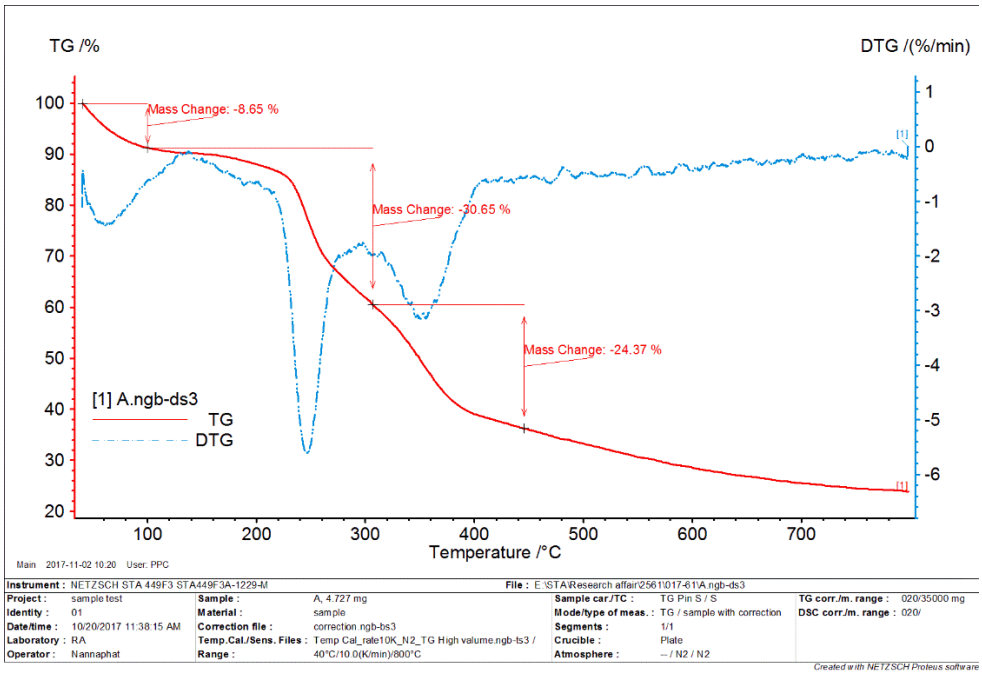

Thermatogram of pEGCG-gum

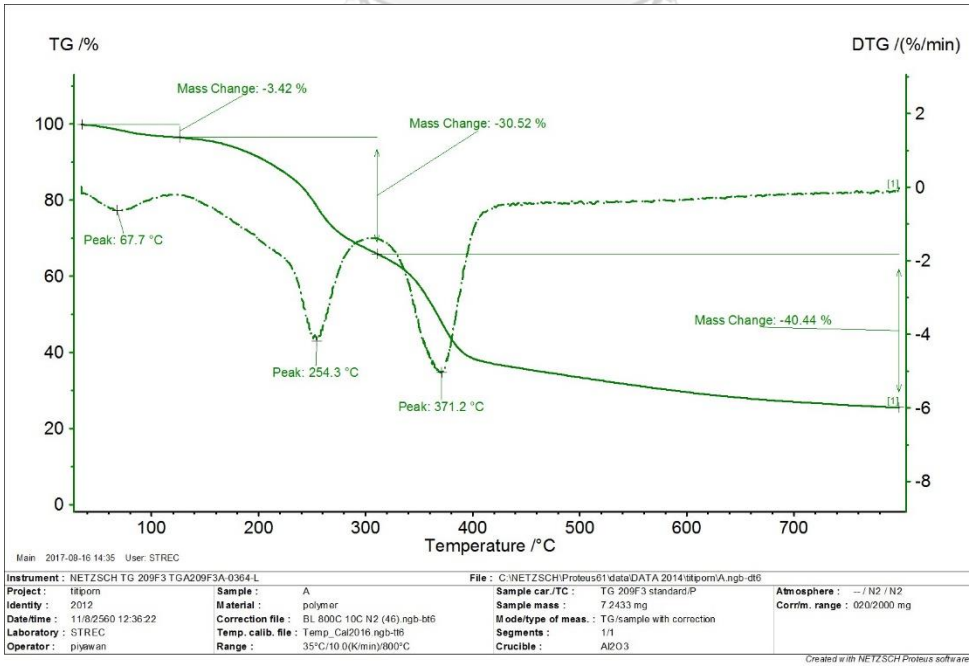

Thermatogram of Fc-pEG II

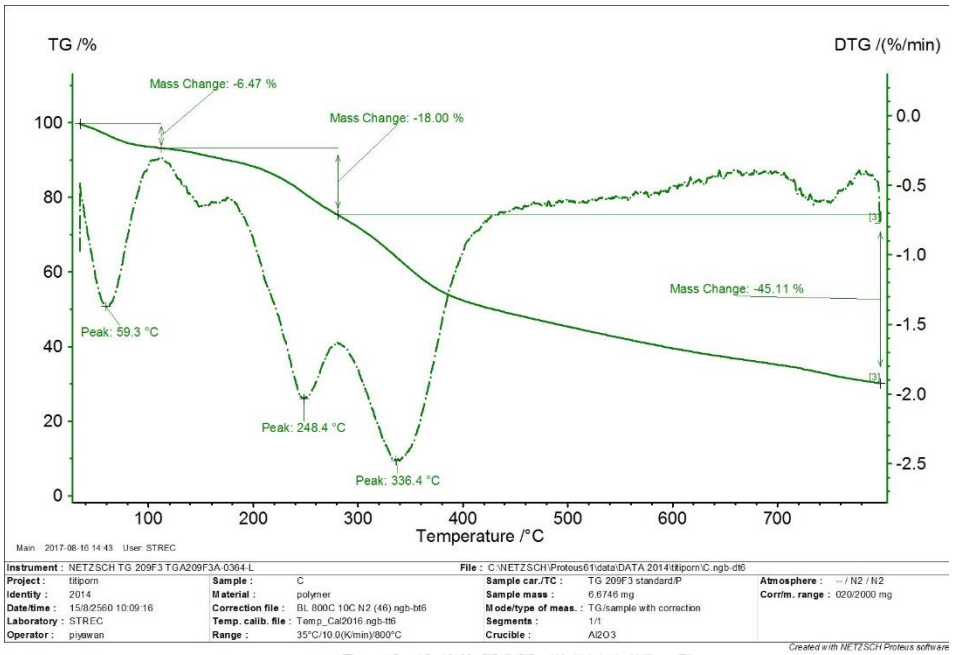

Thermatogram of Fc-pEG-gum

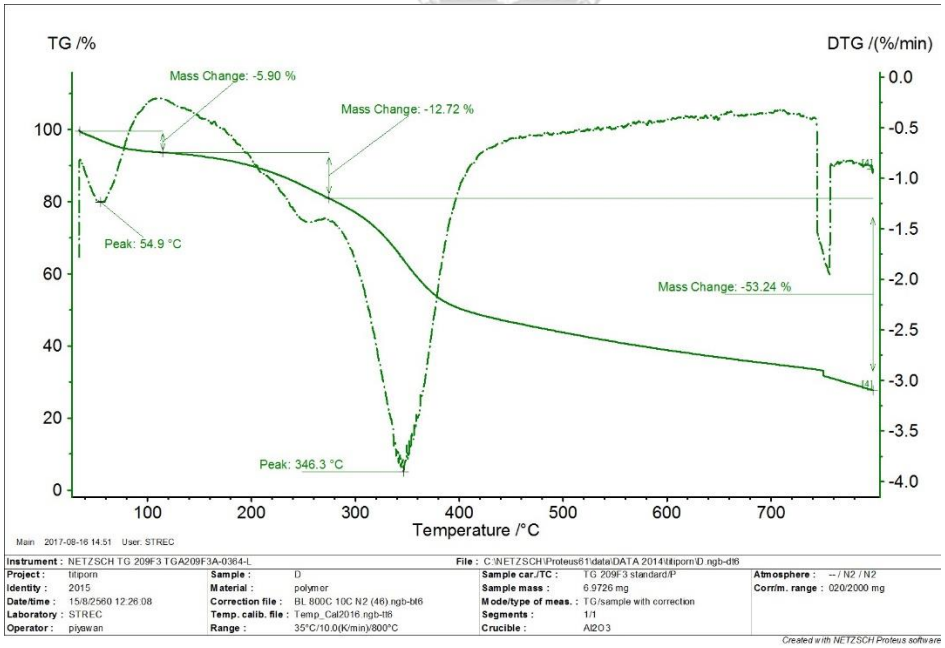

Thermatogram of oxFc-pEG II

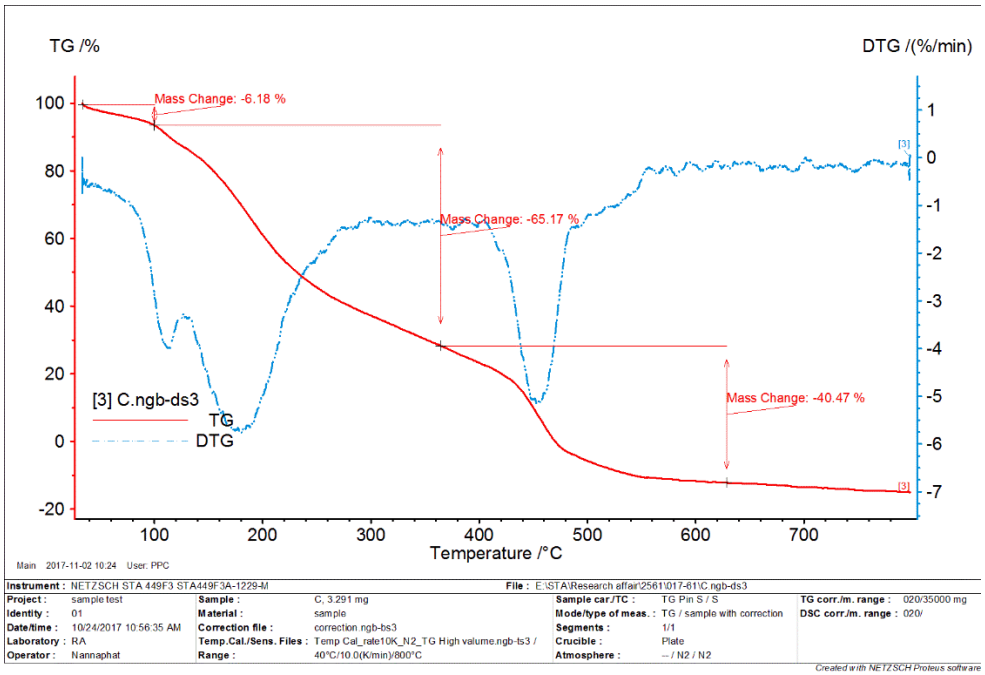

Thermatogram of oxFc-pEG-gum

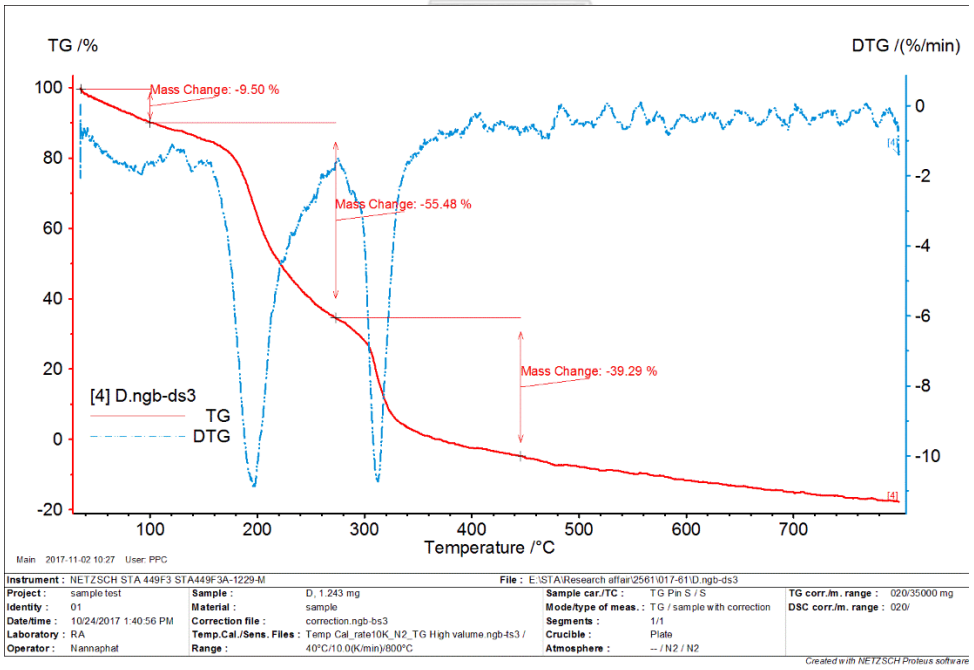

5. Calculation of weight percentage of ferrocene incorporated in the particles

Iron standard curve

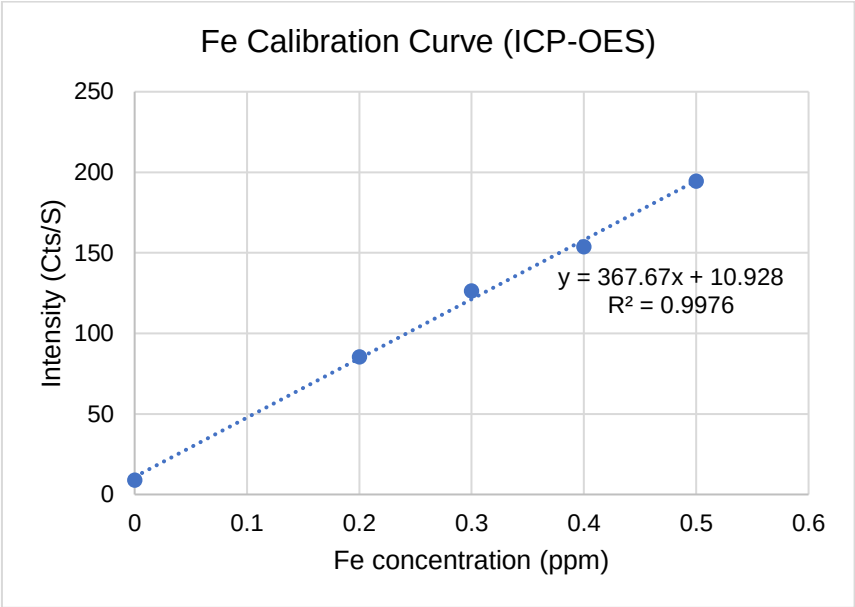

Concentration of iron calculated from iron standard curve

Sample	Iron concentration (ppm)
Fc-pEG I	0.1199
Fc-pEG II	0.1371
Fc-pEG-gum	0.2253
oxFc-pEG I	0.2845
oxFc-pEG II	1.136
oxFc-pEG-gum	1.216

Calculation of weight percentage of ferrocene incorporated in the particles

$$\text{weight percentage}\ (\%) = \text{conc. of iron}\ \left(\frac{\text{mg}}{\text{L}}\right) \times 0.01\ \text{L} \times \frac{186.04\ \text{mg Fe}}{55.8\ \text{mg Ferrocene}} \qquad \text{(Eq. 5)}$$

Sample	particles (ppm)	volume (mL)	particles (mg)	Fe conc. (ppm)	Fe (mg)	Fc (mg)	Fc in particles (%)
Fc-pEG I	2	10	0.02	0.1199	0.001199	0.003955	19.77
Fc-pEG II	10	10	0.1	0.1371	0.001371	0.004522	4.52
Fc-pEG-gum	10	10	0.1	0.2253	0.002253	0.007432	7.43
oxFc-pEG I	2	10	0.02	0.2845	0.002845	0.009384	46.92
oxFc-pEG II	10	10	0.1	1.136	0.01136	0.037472	37.47
oxFc-pEG-gum	10	10	0.1	1.216	0.01216	0.040111	40.11

VITA

Mr. Punnawich Phaiyarin was born on March 18, 1993 in Bangkok Thailand. He graduated with bachelor's degree of science, major in chemistry from Burapha university in 2014 under supervised Assoc. Prof. Dr. Waree Nuangchomnong. He continued his master's degree at department of chemistry, Chulalongkorn university under supervised Prof. Dr. Supason Wanichwecharungruang. In the present, He lives in Chon Buri, his address is 167/1 Bang nang, Phanthong, Chon buri, Thailand.